NASA CR 114560
AVAILABLE TO THE PUBLIC

DESIGN INTEGRATION AND NOISE STUDIES FOR JET STOL AIRCRAFT

AUGMENTOR WING CRUISE BLOWING VALVELESS SYSTEM

Wind Tunnel Investigation of a
14-Percent-Thick Airfoil with
Upper Surface Blowing at High
Subsonic Mach Numbers

By A. S. Mahal and I. J. Gilchrist

SUMMARY

High-speed aerodynamic characteristics of a 14%-thick airfoil with upper surface blowing are presented. An exploratory investigation was conducted in the Boeing Transonic Wind Tunnel over a Mach number range of 0.60 to 0.80. The Reynolds number range, based on airfoil chord, varied with Mach number between 5.0×10^6 to 6.0×10^6.

The results of the investigation indicate that incorporation of upper surface blowing through protruded multilobed nozzles did not impair the drag divergence characteristics of the airfoil. The drag divergence Mach number for the airfoil, at the required cruise lift levels and nozzle thrust conditions, exceeded the design objectives and occurred just above 0.76. The section drag levels at subcritical Mach numbers appeared to be consistent with other transonic airfoils when drag increments due to nozzle lobe wetted area and jet scrubbing were excluded. Comparison of wind-off thrust measurements of the nozzle on the airfoil model with the nozzle-alone configuration indicated jet-scrubbing losses of the order of 1.5% of the gross nozzle thrust.

INTRODUCTION

Task VII of "Design Integration and Noise Studies," contract NAS2-6344, was implemented by The Boeing Company in March 1972 to define a cruise blowing, valveless augmentor wing system for jet STOL aircraft. The cruise blowing system concept, in which

flow control valves are essentially eliminated, requires a major portion of engine fan air to be discharged through multielement lobed nozzles during all modes of airplane flight. During takeoff and landing these nozzles act as a primary jet flow source for the augmentor/jet flap configurations, producing low noise and high augmentation characteristics. In cruise when the flaps are nested, these nozzles (located on the upper surface of the wing as shown in figure 1) stay exposed and continue to exhaust engine fan air.

System design studies in Task VIIA (ref. 1) revealed that a cruise blowing, valveless augmentor wing concept offered significant advantages in airplane system design and low-speed performance. However, practical application would appear to depend on whether satisfactory drag level and drag rise Mach number could be realized with exposed and protruded lobed nozzles. In order to provide this information, Task VIIB was initiated. The scope of this task was limited to a brief exploratory investigation with a main objective to identify whether any major aerodynamic design problem existed. For this purpose an existing quasi-two-dimensional model of a Boeing airfoil was modified to incorporate lobed nozzles for upper surface blowing. The wind tunnel investigation was conducted in the 8- by 12-ft Boeing Transonic Wind Tunnel facility located at Seattle, Washington.

Airfoil drag and lift levels, drag divergence Mach number, and pitching moment characteristics for four nozzle thrust settings were evaluated for the geometrical angle-of-attack range between -2.0° and 6.0°. The results of the investigation are reported herein.

SYMBOLS AND ABBREVIATIONS

C_d section drag coefficient (ref. 4)

C_m section pitching moment coefficient, $\sum_{l.s.} C_p \frac{\Delta x}{c}(0.25 - x/c) - \sum_{u.s.} C_p \frac{\Delta x}{c}\left(0.25 - x/c\right)$

C_n section normal force coefficient, $\sum_{l.s.} C_p \frac{\Delta x}{c} - \sum_{u.s.} C_p \frac{\Delta x}{c}$

C_p pressure coefficient, $\frac{p - p_\infty}{q_\infty}$

C_p, sonic	pressure coefficient corresponding to local Mach number of 1.0
C_v	nozzle velocity coefficient
C_μ	blowing momentum coefficient, $\frac{\dot{w} \cdot V_j}{g\, q \cdot S}$
c	chord of the airfoil, in.
M	Mach number
NPR	nozzle pressure ratio, P_{t_p}/P_∞
P_{t_p}	plenum pressure, lb/ft^2
p	local static pressure at a point on airfoil, lb/ft^2
p_∞	static pressure in undisturbed stream, lb/ft^2
q_∞	dynamic pressure in undisturbed stream, lb/ft^2
R	Reynolds number based on airfoil chord
r	airfoil-leading-edge radius, in.
S	model reference area, ft^2
T	thrust, lb
t	airfoil thickness, in.
V_j	nozzle jet velocity expanded to free-stream conditions, ft/sec
$\dot{w}$	nozzle air weight flow, lb/sec
x	ordinate along airfoil reference line measured from airfoil leading edge, in.
y	ordinate vertical to airfoil reference line, in.
α	angle of attack of airfoil reference line, deg

Subscripts

DD	drag divergence conditions
g	geometric
l.s.	lower surface
u.s.	upper surface
max	maximum

MODEL DESIGN

The design of the wind tunnel model was based on technical objectives which required that a 14%-thick airfoil with cruise blowing nozzles must demonstrate a drag divergence Mach number above 0.75 at a design lift coefficient of 0.40. This corresponds to a drag divergence Mach number of 0.82 for a 25° sweep finite wing. These goals are representative of the STOL airplane cruise requirement as indicated by the Task VIIA studies (ref. 1).

The design of the airfoil shape as shown in figure 2(a) was constrained by the fact that an existing wind tunnel model was modified and incorporated with multi-element lobed nozzles for upper surface blowing. The nozzle geometry consisted of 44 individual vertical lobe nozzles equally spaced along the model span (fig. 2(a)). Each lobe nozzle having a vertical slot height of 0.90 in. and width of 0.10 in. yielded a nozzle array area ratio of 8.18. A detailed sketch of an individual lobe nozzle, indicating significant dimensions, is shown in figure 2(b).

The modifications of the airfoil shape were achieved using a potential flow method described in reference 2 and comprised of three essential steps: First, the upper surface contour was altered to have a pressure recovery starting at about 40% chord. In this way the flow in the vicinity of the nozzles would be locally subsonic for Mach numbers up to and beyond the abrupt drag rise. The "peaky" characteristics of the original leading edge were retained. The term "peaky" refers to the shape of the incompressible pressure distribution, which has a high suction peak at the nose. The fact that this type of pressure distribution and associated airfoil geometry give marked increases in drag divergence Mach number was first noted by Pearcey (ref. 3). The concept has since been widely developed and applied to advanced transonic airfoil designs at The Boeing Company.

The second design change consisted of modification of the trailing edge. The camber of the airfoil in this region was adjusted so that, at its design angle of attack of 1.6°, the airfoil produced desired lift coefficients of 0.40. The final shape of the lower surface resulted in a relatively flat pressure distribution with pressure recovery starting at about 60% chord. While this latter feature was not desirable for an airfoil with a relatively low design lift, it was necessary to accommodate the blowing system plenum chamber. One advantage of the resulting section shape is that it is exceptionally thick in the regions where wing spars would be placed.

The third design change involved local modification to the airfoil upper surface between nozzle lobes (channel area, see figure 2a) and longitudinal shape of the individual lobes. Although the blowing nozzle would be located in a region of overall subsonic flow (that is, downstream of the embedded supersonic region) in the Mach number range of interest, two further steps were taken to minimize any interference due to their presence on the airfoil. First, a fairing was added to the nozzles to give the smoothest possible area distribution. Second, the airfoil upper surface in the channel area was carved out in an attempt to "area rule" the contour. To design the nozzle fairing, the cross-sectional area of the individual nozzle was distributed across the span of the model, and the resulting area distribution was treated as the effective thickness distribution of the airfoil. Downstream of the nozzle exit an estimated displacement due to nozzle jet exhaust was included as increased airfoil thickness. The area distribution upstream of the nozzle was modified by adding thickness until a smooth area distribution was obtained. The effective thickness distribution of the resulting airfoil, designated as Airfoil "A," is shown in figure 3.

Another airfoil configuration, designated Airfoil "B," was also tested to determine the effects of filling the carved portion of the nozzle channel area by a smoother contour on drag level. Effective thickness distribution of Airfoil B is compared with that of Airfoil A in figure 3. The ordinates of both Airfoil A and Airfoil B are tabulated in table I. In addition, ordinates of nozzle lobe upper surface are listed in table II.

TEST PROGRAM

WIND TUNNEL

The experimental data presented in this report was obtained in the 8- by 12-ft Boeing Transonic Wind Tunnel (BTWT). This tunnel is a continuous, closed-circuit wind tunnel with total pressure in the test section approximately equal to atmospheric pressure. The test

section with longitudinal slots on the walls allows testing through the transonic speed range with minimum wall interference. The model was mounted vertically in the test section floor, its lower end attached to a turntable situated in a solid splitter plate, as shown in figure 4. The function of the splitter plate was to reduce boundary layer thickness in the vicinity of the model and also to provide a reflection plane. A circular end plate with a 40-in. diameter was mounted at the top of a 20-in. constant chord model with 36-in. span to produce a quasi-two-dimensional environment. Figure 5 shows the test section with model installed. During each test run the tunnel Mach number was maintained within ±0.002 of the prescribed nominal value. The model was pitched through a series of specified angles of attack by means of remotely controlled hydraulic actuators. At each angle the test section flow was allowed to stabilize before pressure measurements were recorded. Throughout each run the nozzle pressure ratio was remotely controlled and adjusted to maintain a prescribed value of momentum coefficient, C_μ.

TRANSITION STRIPS

Boundary layer transition was fixed by means of a single row of point disturbances on each surface, located along the 10% chordline. These disturbances were generated by cylindrical discs spaced at intervals of 0.4 in., projecting from the airfoil surface. The discs were glued to the model and had a thickness (trip height) of 0.005 in., determined according to the method of reference 4. The diameter of the discs was 0.062 in. Use of discs has been found to be very helpful in achieving uniform transition along the span and has been a standard technique in airfoil testing at Boeing.

DATA ACQUISITION AND REDUCTION

Lift and Pitching Moments

The normal force and pitching moments acting on the model were calculated from surface pressure distributions. Surface pressures were measured at the semispan station of the model from 60 chordwise pressure orifices. The orifices were concentrated near the leading edge and other selected regions of the airfoil for better definition of severe pressure gradients. Pressures were measured by means of a scanning valve and a differential pressure transducer referenced to tunnel total pressure. The section normal force coefficient, C_n, and pitching moment coefficient at quarter chord point, C_m, were computed by integration of local pressure coefficients, C_p, measured at each orifice and multiplied by an appropriate weighting factor. The contributions of nozzle jet reactions to lift were considered to be very

small (less than 2% at $C_n = 0.40$ and $C_\mu = 0.044$) and therefore were neglected. However, in the case of pitching moments the increments due to nozzle thrust reaction were included as the contributions were sizable (approximately 10% of total C_m).

Drag

The drag forces acting on the airfoil were obtained from horizontal variation of static and total pressures in the wake at the semispan station of the model. These variations were measured with a five-probe total pressure rake and a single static pressure probe mounted on a traversing mast which aligned itself with local flow, thus keeping flow angularity errors to a minimum. Pressures at each probe were measured on separate differential transducers, referenced to the tunnel total pressure. Probe position was recorded by means of a well-calibrated potentiometer. The measurement station of the rake was approximately 0.85 chord length behind the trailing edge of the airfoil. All five total head probes (spaced 0.40 in. apart) measured nearly the same drag values thereby indicating complete mixing of jet and wake by the time flow reached the measuring station. For data presentation, an average of all five total head probes has been used.

Blowing parameters such as momentum coefficient, C_μ, were obtained from measurements of nozzle exhaust weight flow, $\dot{w}$, and total pressure conditions in the model plenum. High-pressure air was continuously metered through an ASME nozzle upstream of the model plenum. Total pressure and temperature probes were located in the plenum for calculation of ideal jet velocity, V_j.

To obtain a section drag coefficient, C_d, deficiency of momentum within the wake was computed by the method of reference 5 and multiplied by appropriate weighting factors. Drag values determined from wake measurements included thrust contributions, and for isolating these effects nozzle jet thrust components were subtracted for data presentation.

Angle-of-Attack Correction

Due to quasi-two-dimensional features of the model, the real aerodynamic angle of attack is significantly lower than geometric angle. Correction to the angle of attack takes the form

$$\alpha = \alpha_g - K C_n$$

where the parameter K is a function of the effective aspect ratio of the model which varies with Mach number, model geometric aspect ratio, and the diameter of the end plate.

Analysis of the model with end plate using the method of reference 6 indicated that the effective aspect ratio of the model is approximately five. On the basis of analysis and tunnel flow characteristics, the value of K is determined by the following relation:

$$K = 3.537 - 1.256\sqrt{1 - M^2}$$

TEST CONDITIONS

The experimental investigations were conducted over a Mach number range of 0.60 to 0.80. The Reynolds number of the test based on model chord varied with Mach number over a range of 5.09×10^6 to 5.92×10^6 (fig. 6). The nozzle blowing momentum coefficients were varied from 0 to 0.045. The geometric angle of attack varied from -2.0° to 6.0°. The total temperature of the tunnel was held constant at approximately 610° R.

RESULTS

The results of this investigation have been reduced to coefficient form. Selected data representing these results are presented in the figures listed below:

DISCUSSION

DRAG RISE CHARACTERISTICS

Drag variations with Mach number for Airfoil A at constant C_n conditions are shown in figure 7 for four nozzle blowing settings, namely: C_μ = 0, 0.017, 0.028, and 0.044. Drag is shown in terms of $C_d + C_\mu$ to isolate thrust contributions. The results presented in figure 7 indicate that for a design C_n of 0.40 the drag divergence (defined when $\partial(C_d + C_\mu)/\partial M = 0.1$) occurs above the design objective Mach number of 0.75 for all blowing rates. Furthermore, examination of data in figure 8 shows that drag divergence Mach number

increases with increasing values of blowing momentum coefficients for all levels of lift investigated during the test. In fact, the increment in drag divergence Mach number due to blowing substantially improves with increasing lift levels. At the design C_n of 0.40 the drag divergence for the unblown condition occurs at a Mach number of 0.754. With nozzle blowing conditions at C_μ of 0.044 the abrupt drag rise is delayed to the Mach number of 0.762.

Oil flow photographs (fig. 9) taken at a fixed geometric angle of 4° and a C_μ of 0.044 show that movement of the shock wave with increasing Mach numbers is typical of "peaky" type airfoil technology. At low Mach numbers the supercritical region is confined to the leading edge area due to intentionally designed high suction peaks. This can be observed in the photograph taken at Mach number 0.70, where the shock is located between 15% and 20% chord stations. Near the design Mach numbers the embedded supersonic region expanded downstream, with the terminating shock located just ahead of the nozzle fairings as seen in the M = 0.74 photograph. Above drag divergence Mach numbers (M = 0.76), the shock moved slightly into the channel part of the nozzle but shows no signs of flow separation. This indicates that drag rise characteristics of Airfoil A are mainly associated with energy losses in the terminating shock. Flow separation on the airfoil did not occur until the Mach numbers were well beyond drag rise values. This is evident from the photograph taken at M = 0.78, (ΔM of 0.04 above drag divergence), where the oil flow pattern indicates nonuniformity due to flow separation.

The phenomena associated with drag rise of Airfoil A are also portrayed by the pressure distributions shown in figure 10, where it can be clearly noted that just below the drag divergence Mach number (M = 0.74) the terminating shock is ahead of the nozzle fairings and final pressure recovery is well behaved. Even at a Mach number of 0.76 ($\Delta M \approx 0.02$ above drag rise) for lift levels below $C_n = 0.40$ the final pressure recovery shows no signs of flow separation despite the fact that local Mach numbers are above 1.3, where wave drag is known to increase very rapidly with increasing Mach numbers. At all Mach numbers below drag divergence the flow over the nozzle channel length and downstream has been subsonic. Oil flow photographs and pressure distributions in the channel area indicate well-behaved flow between the nozzle lobes, with no visible separation present.

VARIATIONS WITH BLOWING RATES

Due to the exploratory nature of the experimental investigation, the nozzle blowing rates were confined to four nominal settings for all Mach numbers. These were C_μ of 0.017, 0.028, 0.044, and the unblown condition ($C_\mu = 0$).

Examination of the lift data in figure 11 shows sizeable increases in lift levels with increasing blowing rates at constant angles of attack. These increases, as expected, are associated with the jet flap effect of upper surface blowing, which creates supercirculation. The evidence of increasing lift with increasing blowing rate is also provided by the pressure distributions in figure 12, where one notices indication of flow separation as the $C_\mu = 0$ condition and marked changes in shock location, lower surface pressure distributions, and improved upper surface pressure recovery with blowing-on conditions. It is interesting to note that the change in shock location and strength for increase in C_μ from 0.028 to 0.044 was quite negligible in spite of the fact that the lift level changed from C_n of 0.52 to 0.58.

At a design normal force coefficient of 0.40, the variations in effective drag ($C_d + C_\mu$) with nozzle thrust at and below the drag divergence Mach number in figure 13 show that drag levels at thrust-off conditions are highest. The presence of a nonblowing lobed nozzle causes flow separations on the upper surface. When the nozzle air is turned on, the drag level initially drops until flow separation is eliminated and then assumes a shallow linear rise with further increases in blowing rates. Assuming ideal nozzle flows and no interference drag, thrust losses of the order of 5.25% are noted in the linear portion. These losses mainly consist of:

- Nozzle internal losses
- Jet momentum loss due to scrubbing on the upper surface of the airfoil downstream of nozzle exit
- Section profile drag increment due to change in blowing rate, which may have been charged as thrust loss

At wind-on conditions the isolation of the above-mentioned losses from the total airfoil drag was not possible. Therefore, to assess the order of magnitude of nozzle internal losses and jet scrubbing losses, the model was installed on an external balance, and static thrust measurements with varying plenum pressure level were made. Along with thrust measurements, nozzle air weight flows and nozzle exit total pressures were also recorded. On the basis of these measurements nozzle velocity coefficients, C_v, at various nozzle pressure ratios were computed, and the variations of C_v, weight flow, and nozzle gross thrust, T, with nozzle pressure ratio are presented in figure 14. The velocity coefficient is shown in a wide band of 0.01 to 0.02 ΔC_v. This represents data scatter in weight flow, thrust, and nozzle exit total pressure measurements. The nozzle velocity coefficient at design nozzle pressure ratio of 2.7 is about 0.965, which is about 1% lower than comparable static test data of Task VIIC of the "Design Integration and Noise Studies" program.

In addition, nozzle-alone thrust was also measured by isolating the nozzle from the airfoil assembly to determine jet scrubbing losses. The balance measured thrust with and without the scrubbed surface is compared in figure 15. The balance measurements showed scrubbing loss less than 1.5% of the gross thrust, which approached the range of data scatter.

The sum of nozzle internal losses and external jet scrubbing losses almost accounts for the total thrust recovery loss observed in figure 13. However, it is emphasized that with wind-on these losses are apt to change slightly. The drag data at subcritical Mach numbers ($M < 0.7$) in figure 7d shows that at the design lift conditions ($C_n = 0.4$) the airfoil total drag level is about 0.015 when nozzle ideal thrust is subtracted from the measured value. Further exclusions, of estimated nozzle internal losses ($\Delta C_d \approx 0.0015$), jet scrubbing loss ($\Delta C_d \approx 0.0007$) and parasitic drag increment due to nozzle lobes ($\Delta C_d \approx 0.003$) from the measured drag level indicate that the basic drag level of the airfoil ($C_d \approx 0.0098$) for the above conditions compares well with the data of reference 7. This implies that presence of a vertical lobe causes practically no interference drag penalty at the low Mach numbers.

In figure 13 the changes in section pitching moments with varying blowing conditions are also presented. Pitching moments assumed more negative values with increasing nozzle thrust, which is quite consistent with the jet flap theory. Variations in section pitching moments, at C_n of 0.40, with Mach number are also shown in figure 16 for blowing momentum coefficients of 0.028 and 0.044. Pitching moment levels appear to fall within the range of other airfoil data, and variations with Mach numbers show expected trends.

NOZZLE CHANNEL AREA VARIATIONS

A brief investigation of the effects of airfoil upper surface contour change in the nozzle channel area on the drag characteristics was conducted. The contour change involved filling up the carved-out portion of the Airfoil A upper surface in the channel area along a smooth contour (designated as Airfoil B) to provide additional duct volume for system design.

The comparison of the Airfoil A and Airfoil B drag data for a C_μ level of 0.028 is presented in figure 17(a). It shows that at the drag divergence Mach numbers of Airfoil A the drag level of both airfoils is practically the same. However, at the lower Mach numbers ($M \approx 0.70$) the drag level of Airfoil B is higher than that of Airfoil A, and the difference increases with increasing lift levels. At the design lift conditions ($C_n = 0.40$) the drag level of Airfoil B is roughly six counts above that of Airfoil A.

The effects of contour changes on the local pressure distribution are presented in figure 17 (b), where it is noted that differences are almost negligible in the supercritical flow regions but are quite distinguishable in the channel area. The aft recovery of Airfoil B moved 10% chord aft of Airfoil A and becomes more steep. The same drag level near drag rise Mach numbers can be explained by the observation of pressure distribution data, which shows that though aft recovery of Airfoil B is more severe than that of Airfoil A, the shock strength of Airfoil B appears to be lower than that of Airfoil A and could be an offsetting factor.

CONCLUSIONS

A wind tunnel test has been conducted at Mach numbers from 0.60 to 0.80 to investigate the effects of upper surface cruise blowing on the aerodynamic characteristics of a 14%-thick airfoil. Results of this investigation indicate the following general conclusions for the airfoil lift and thrust levels corresponding to the cruise conditions of a STOL airplane:

(1) The drag divergence Mach number of the airfoil exceeds the design objective and occurs above a Mach number of 0.76.

(2) The drag level of the airfoil at subcritical Mach numbers is in the range of other transonic airfoils, when nozzle internal losses, jet scrubbing losses, and parasite drag increment due to nozzle lobes are excluded.

(3) Thrust losses due to jet scrubbing on the upper surface of the airfoil are of the order of 1.5%.

(4) Filling up of carved surface in the nozzle channel area does not deteriorate the drag divergence characteristics, but the drag level at lower Mach number goes up by approximately 4%.

(5) Finally, it can be stated that the augmentor wing cruise blowing concept is aerodynamically sound and can meet the high-speed performance objectives set forth by Task VIIA studies (ref. 1).

Boeing Commercial Airplane Company
P. O. Box 3707
Seattle, Washington 98124
January 5, 1973

REFERENCES

(1) Design Integration and Noise Studies for Jet STOL Aircraft, Task VIIA: Report on Design Exploration of Augmentor Wing Cruise Blowing Valveless System. D6-40829, Boeing Commercial Airplane Company, October 1972.

(2) Devenport, F.J.: Singularity Solution to General Potential Flow Airfoil Problems. D6-7202, Boeing Commercial Airplane Company, May 1963.

(3) Pearcey, H. H.: The Aerodynamic Design of Section Shapes for Swept Wings, Advances in Aeronautical Sciences, Vol. 3. Pergamon Press, Inc., 1962.

(4) Braslow, A. L.; and Knox, E. C.: Simplified Method for Determination of Critical Height of Distributed Roughness Particles for Boundary-Layer Transition at Mach Numbers from 0 to 5. NACA TN 4363, 1958.

(5) Lock, C. N. H.; Hilton, W. F.; and Goldstein, S.: Determination of Profile Drag at High Speeds by a Pitot Traverse Method. Reports and Memoranda 1971, Brit. A.R.C., 1945.

(6) Rubbert, P. E. and Saaris, G. R.; "Review and Evaluation of a Three-Dimensional Lifting Potential-Flow Analysis Method for Arbitrary Configurations." AIAA paper 72-188, presented at AIAA 10th Aerospace Sciences Meeting, January 17-19, 1972.

(7) Royal Aeronautical Society Data Sheets, Aerodynamics, Wings 02.04.02, Brit., March 1957.

Table 1.—Airfoil A and B Surface Ordinates (c = 20 in.)

x/c	y/c		
	Upper airfoil A	Upper airfoil B	Lower airfoil A and B
0	0	0	0
0.0075	0.02278	0.02278	-0.01941
.0125	.02740	.02740	- .02380
.0250	.03445	.03445	- .03100
.0375	.03920	.03920	- .03620
.050	.04320	.04320	- .04011
.075	.04930	.4930	- .04590
.100	.05461	.05461	- .05002
.125	.05890	.05890	- .05310
.15	.06270	.06270	- .05540
.20	.06840	.06840	- .05890
.25	.07290	.07290	- .06090
.30	.07598	.07598	- .06175
.35	.07821	.07821	- .06206
.40	.07924	.07924	- .06168
.45	.07886	.07886	- .06066
.50	.07701	.07701	- .05897
.55	.07368	.07368	- .05650
.60	.06830	.06903	- .05307
.65	.06086	.06337	- .04834
.70	.05198	.5705	- .04194
.74	.04589	.05167	- .03548
.76	.04420	.04884	- .03190
.78	.04361	.04601	- .02786
.80	.04280	.04310	- .02375
.82	.04009	.04009	- .01931
.86	.03391	.03391	- .01044
.90	.02748	.02748	- .00238
.95	.01906	.01906	.00531
.98	.01381	.01381	.00825
1.00	.01022	.01022	.00941
Leading edge radius = 0.031 c			

Table 2.—Nozzle Upper Surface Ordinates

x/c	y/c
0.40	0.07924
.45	.08125
.50	.08300
.55	.08552
.60	.08975
.65	.09600
.70	.10232
.72	.10275
.74	.10158
.76	.09900
.78	.09500
.805	.08800

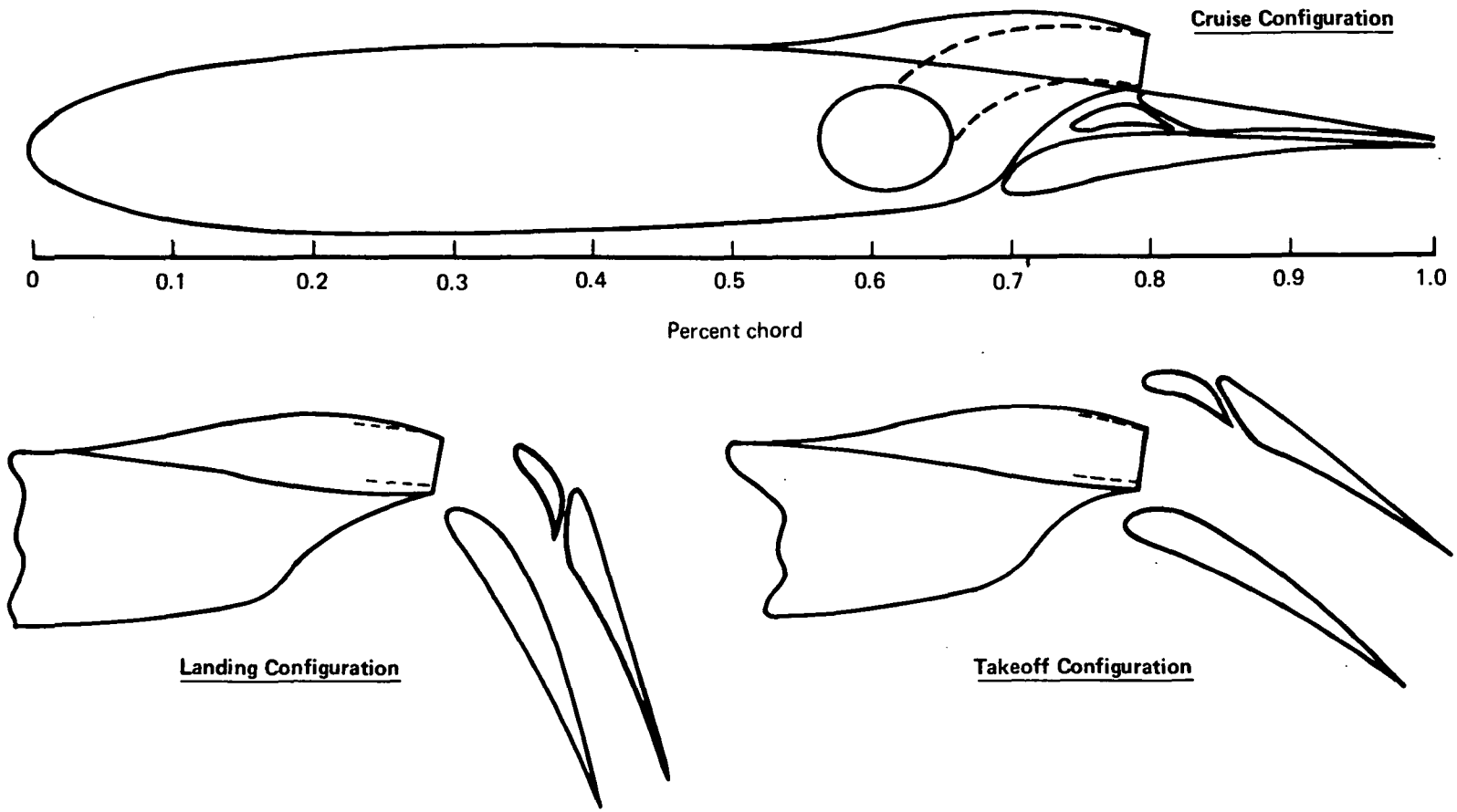

Figure 1.—Cruise Blowing Augmentor Concept

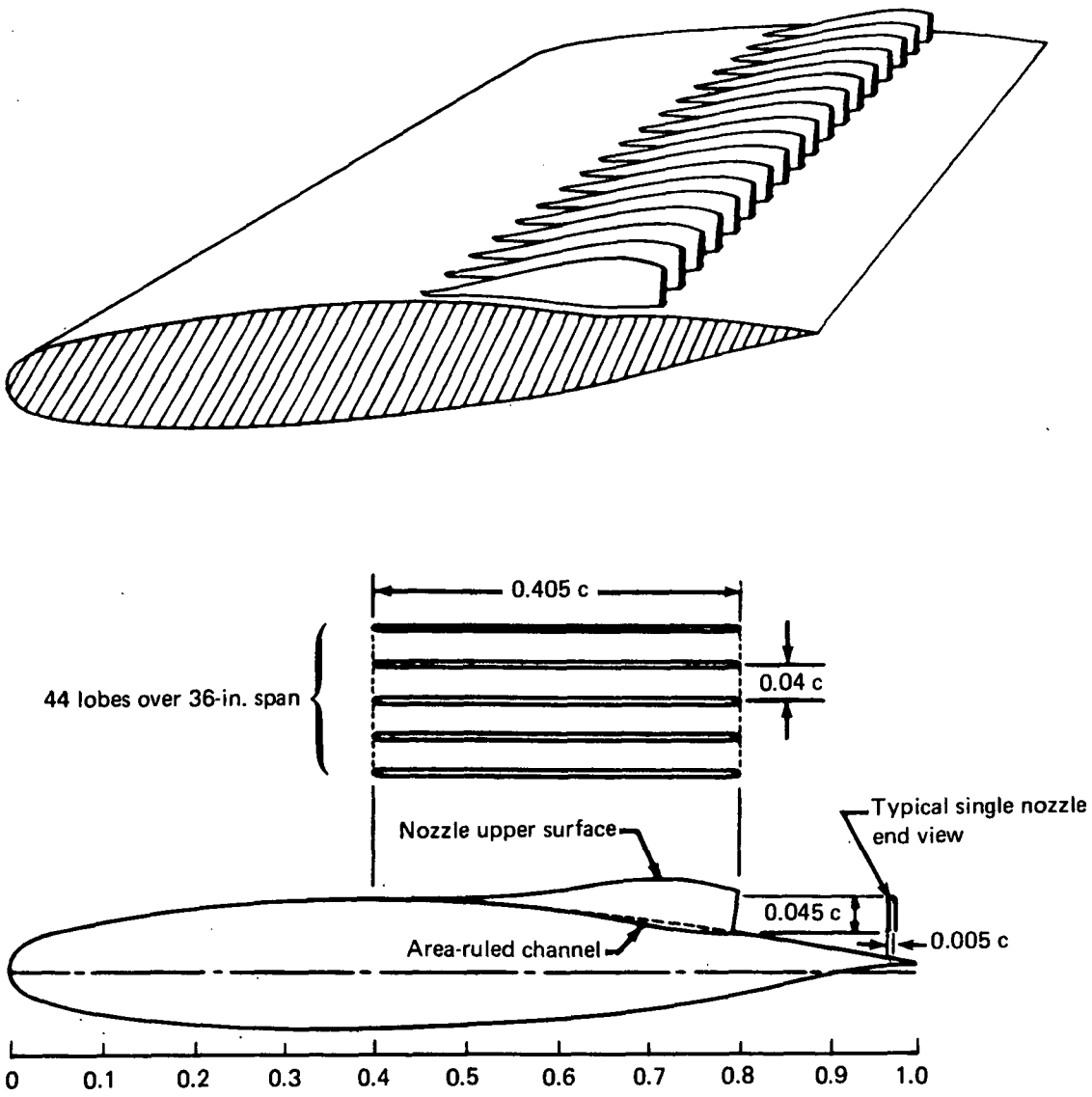

Figure 2(a).—Airfoil Section Shape With Multilobe Nozzle Arrangement

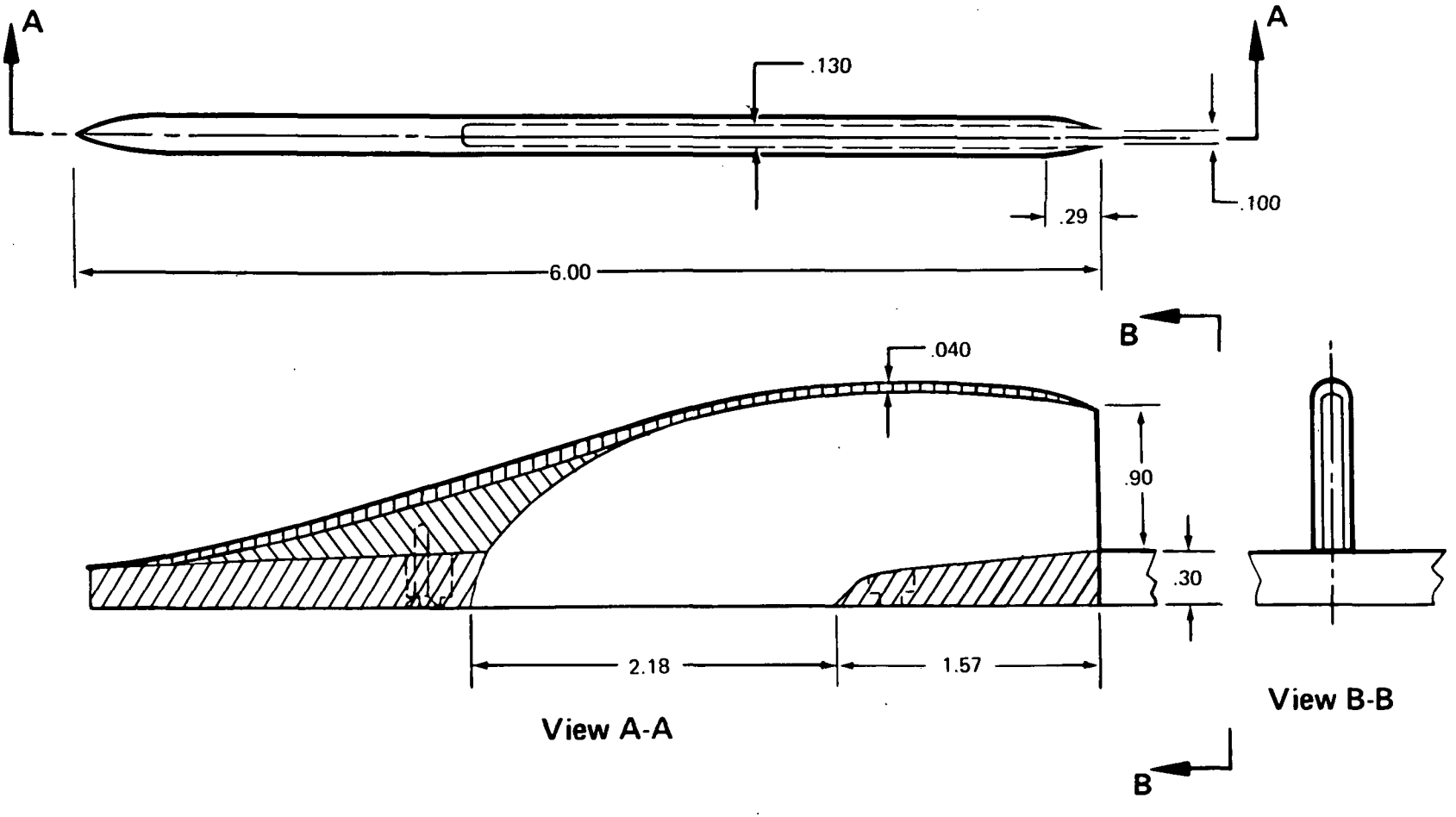

All dimensions are in inches

FIGURE 2b.– LOBE NOZZLE DETAIL

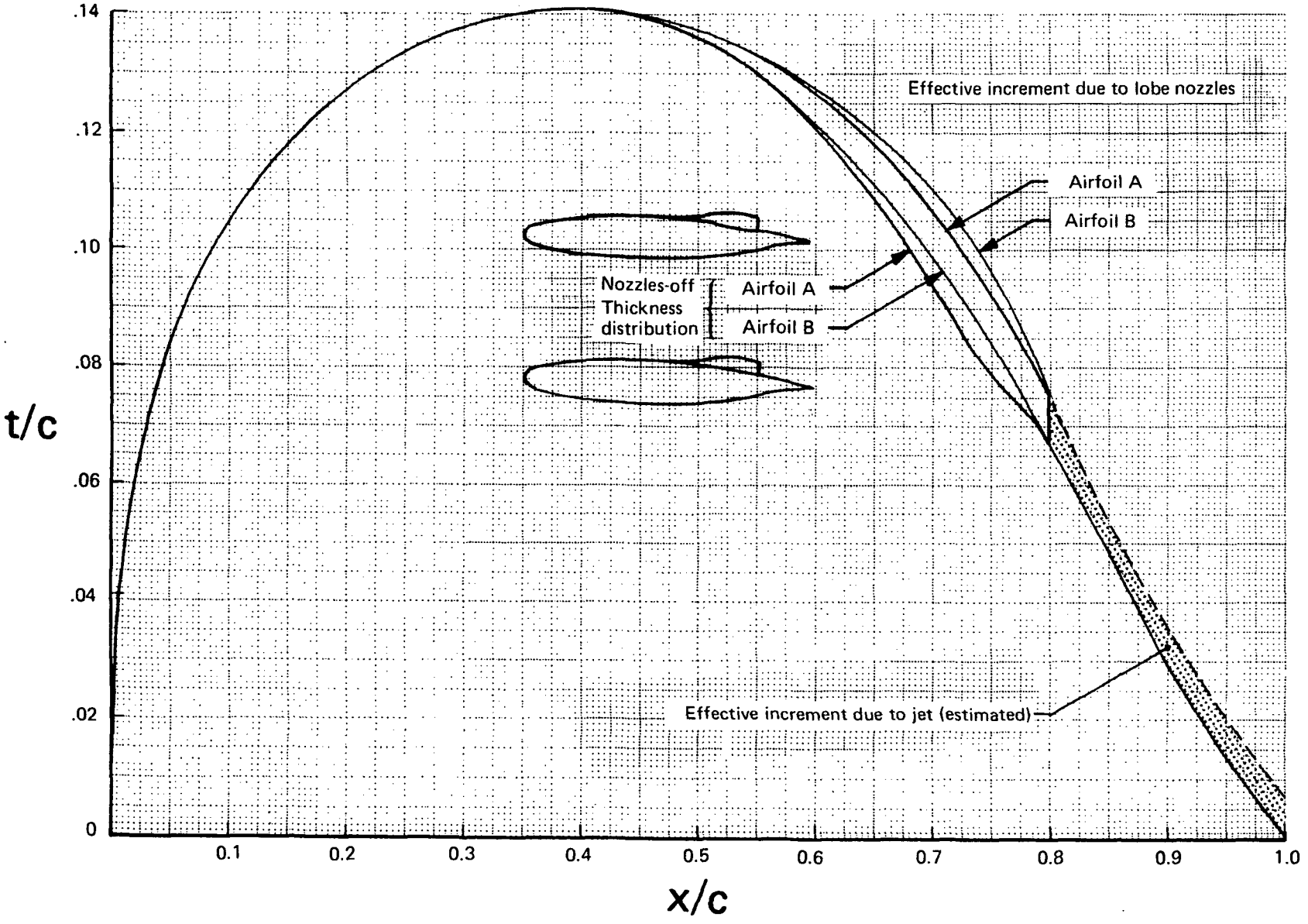

Figure 3.—Airfoil Effective Thickness Distribution Including Nozzle and Contour Channel Increments

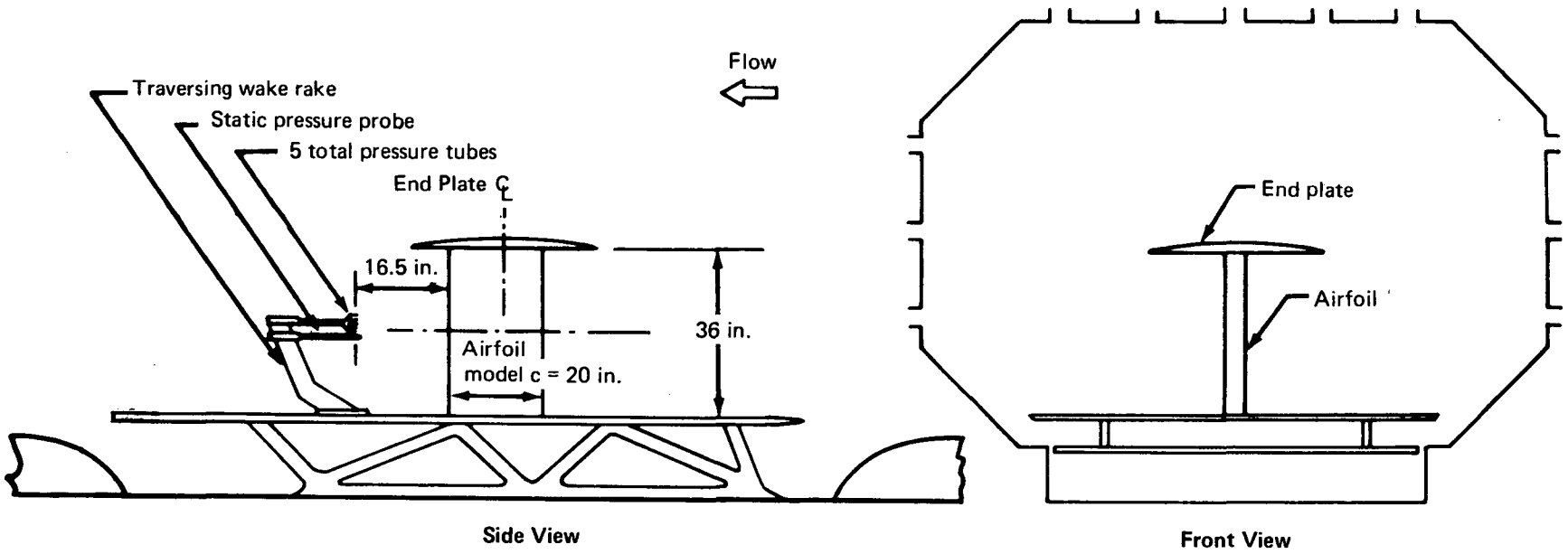

Figure 4.—Quasi-Two-Dimensional Test Setup in Boeing Transonic Wind Tunnel

(a) Model Installation

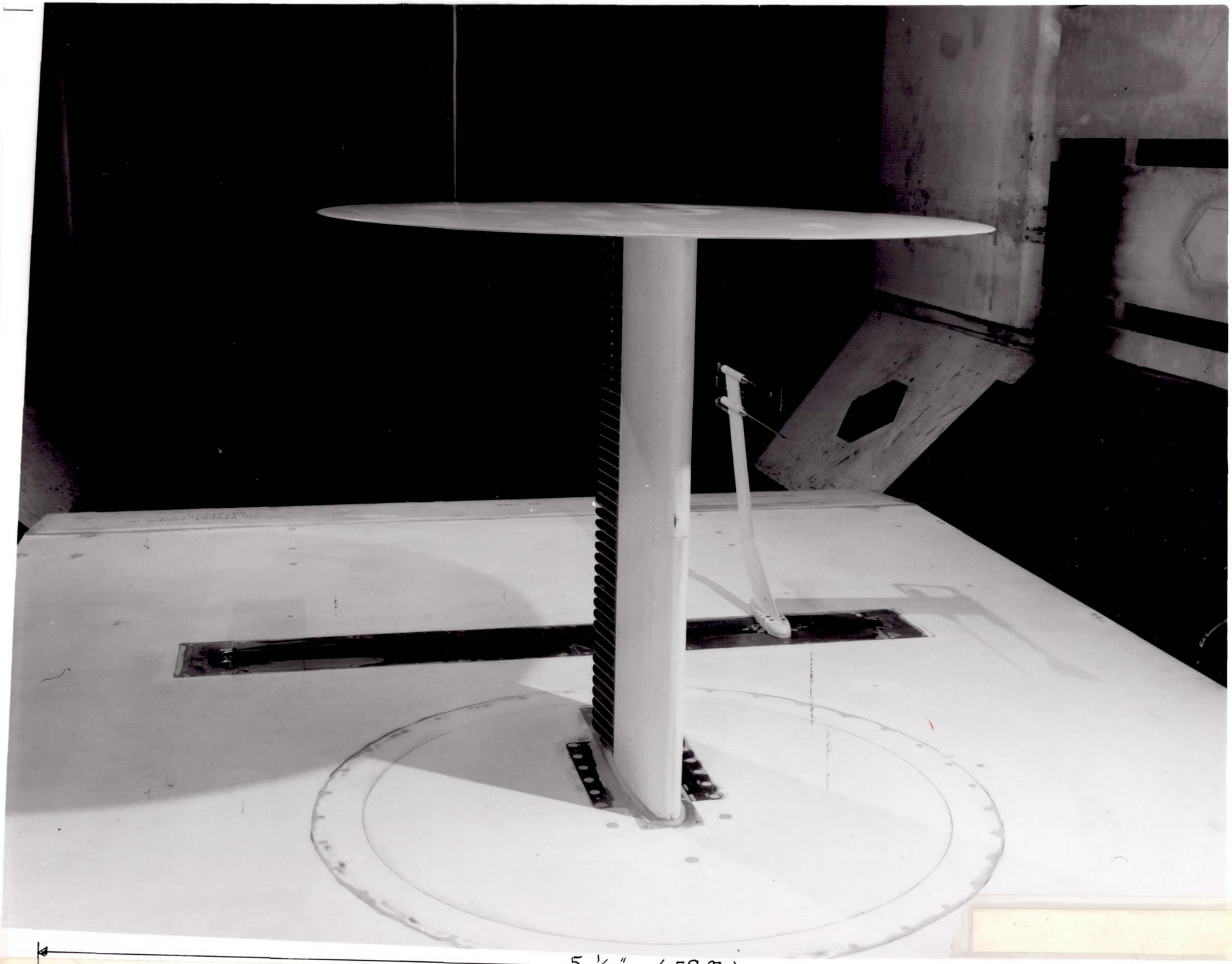

Figure 5 – Cruise Blowing Airfoil Model in the Wind Tunnel

Figure 5 – Cruise Blowing Airfoil Model in the Wind Tunnel

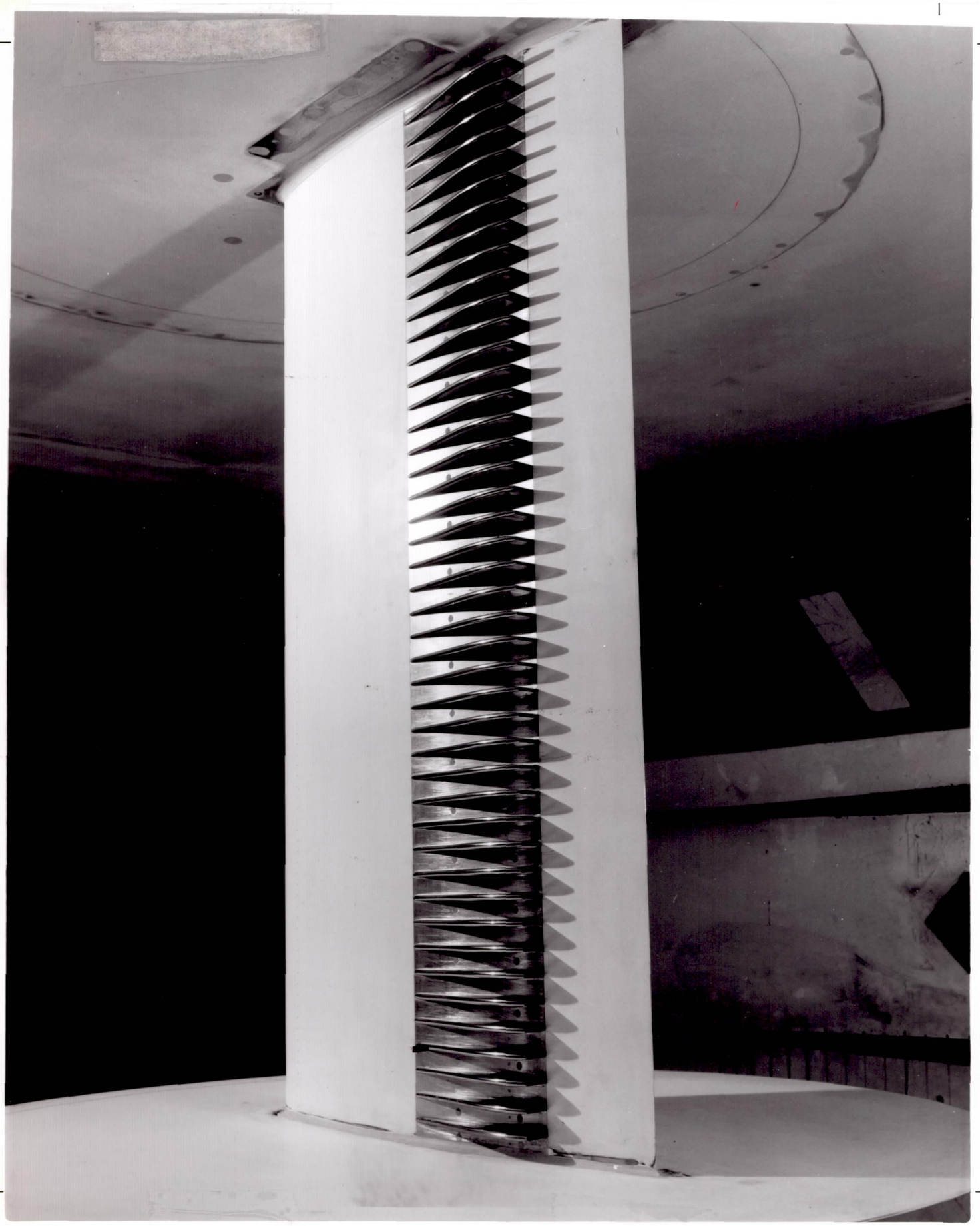

(b) Nozzle Arrangement

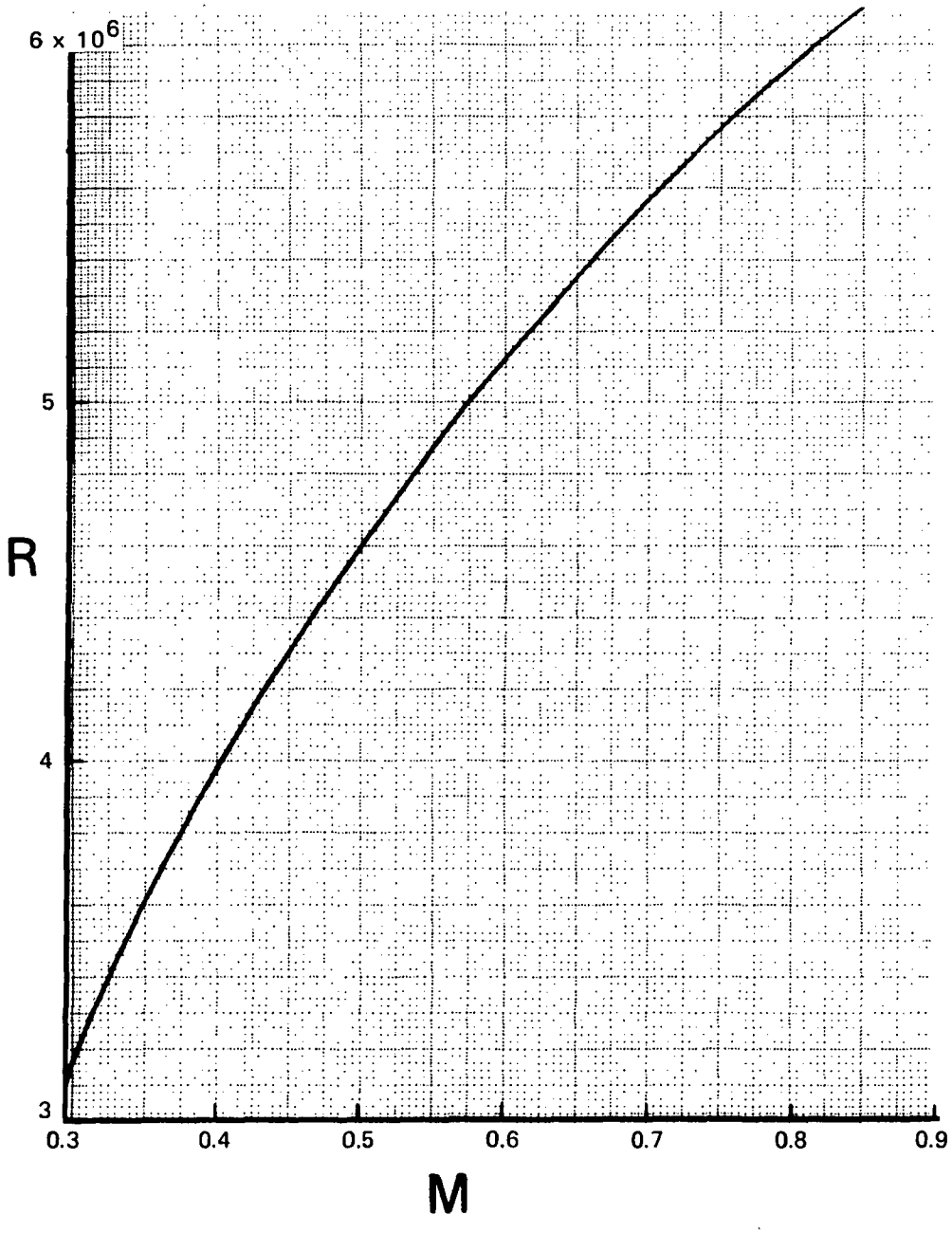

Figure 6.—Variation With Mach Number of Test Wind Tunnel Reynolds Number Base on Airfoil Chord of 20 In.

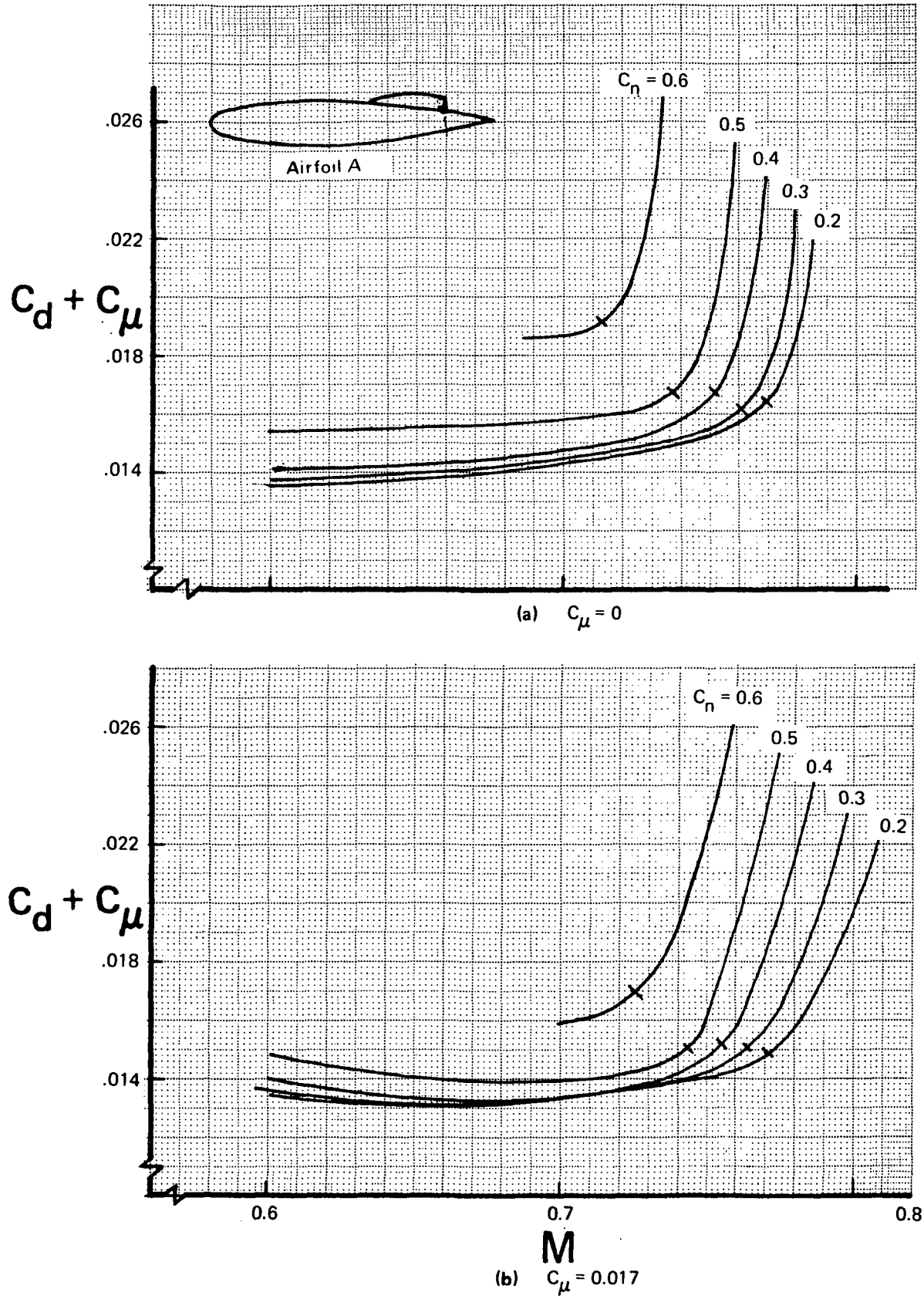

Figure 7.—Variation of Section Drag Characteristics With Mach Number for Constant Value of Section Normal Force and Blowing Momentum Coefficients

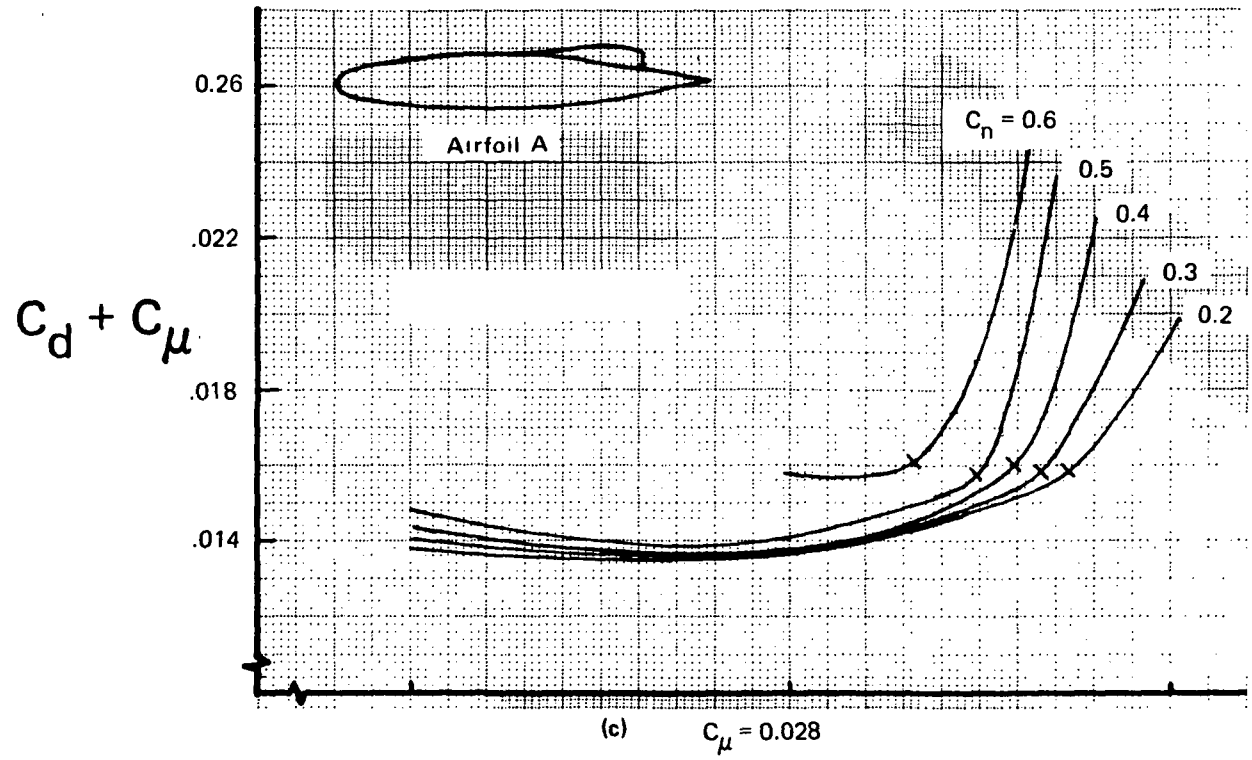

(c) C_μ = 0.028

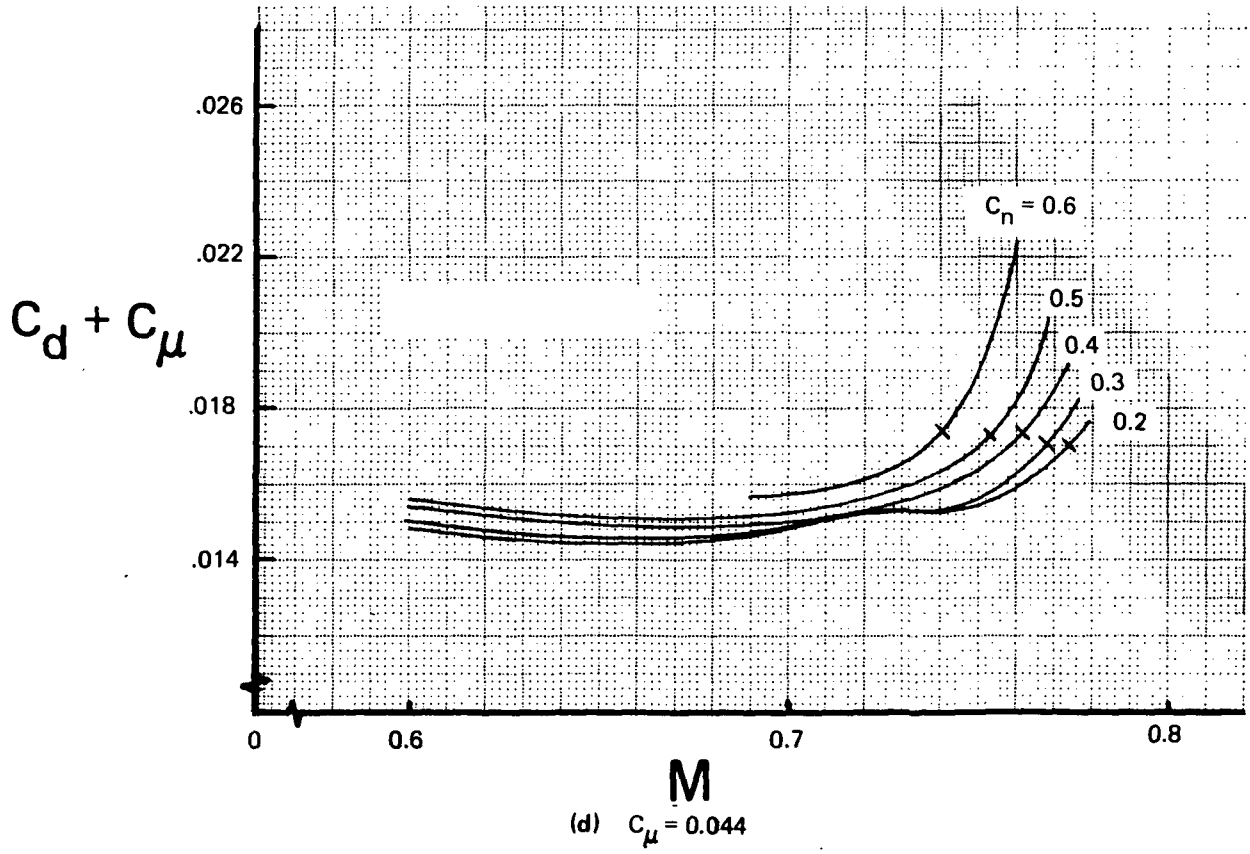

(d) C_μ = 0.044

Figure 7.—Concluded

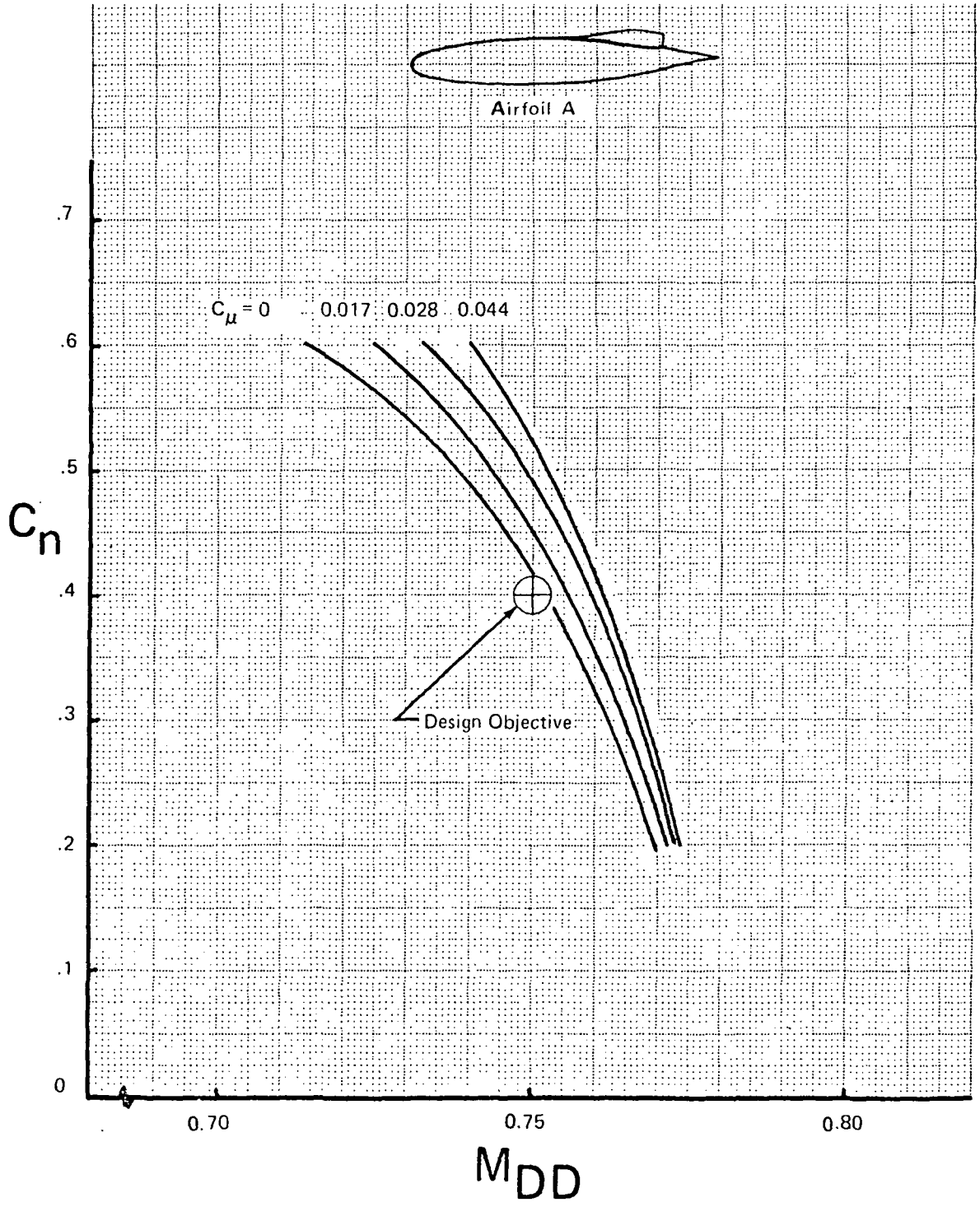

Figure 8.—Variation of Section Normal Force Coefficient With Drag Divergence Mach Number

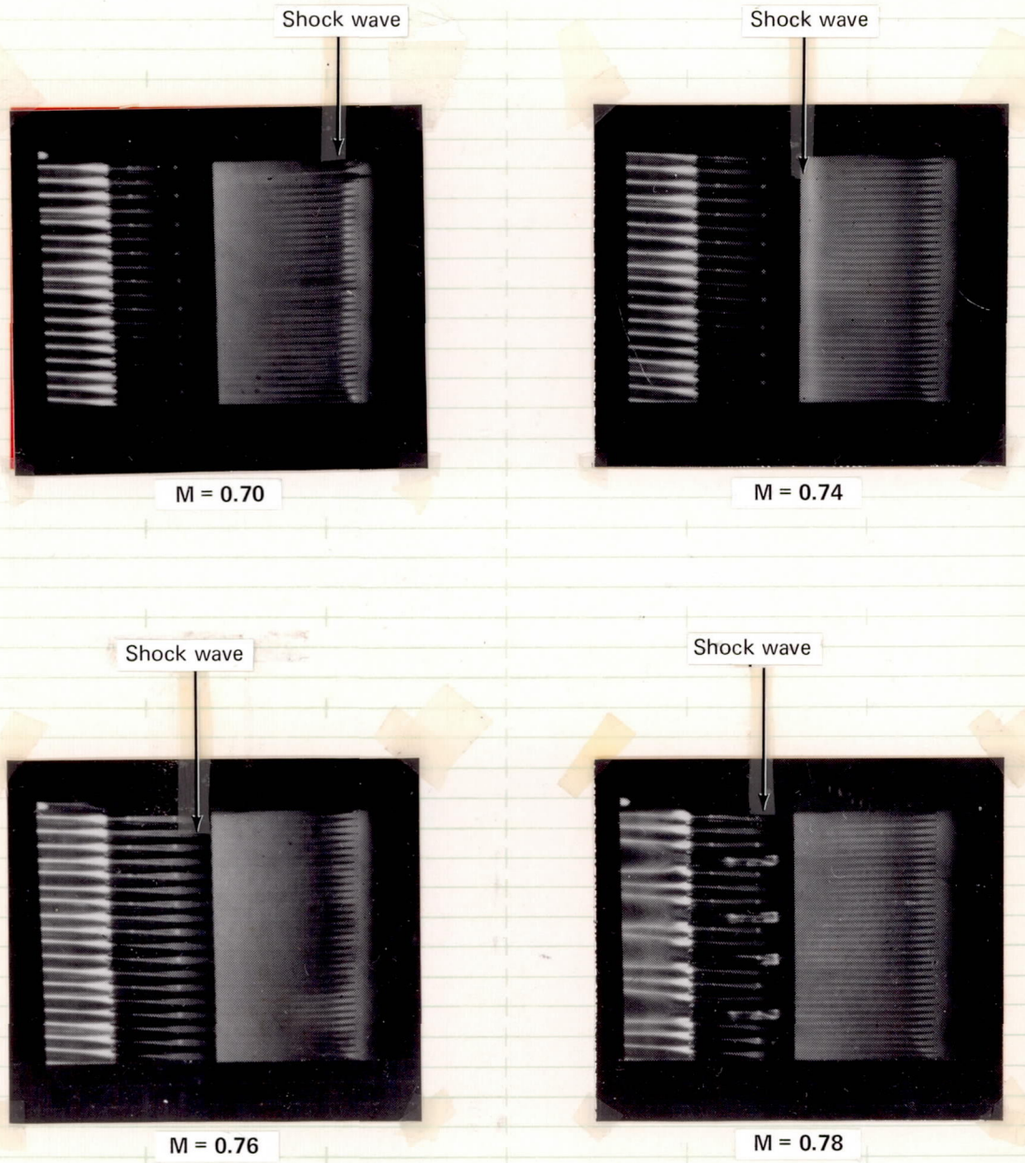

Figure 9.—Oil Flow Photographs at Geometric Angle of Attack of 4° For Mach Numbers From 0.70 to 0.78 at Blowing Momentum Coefficient of 0.044

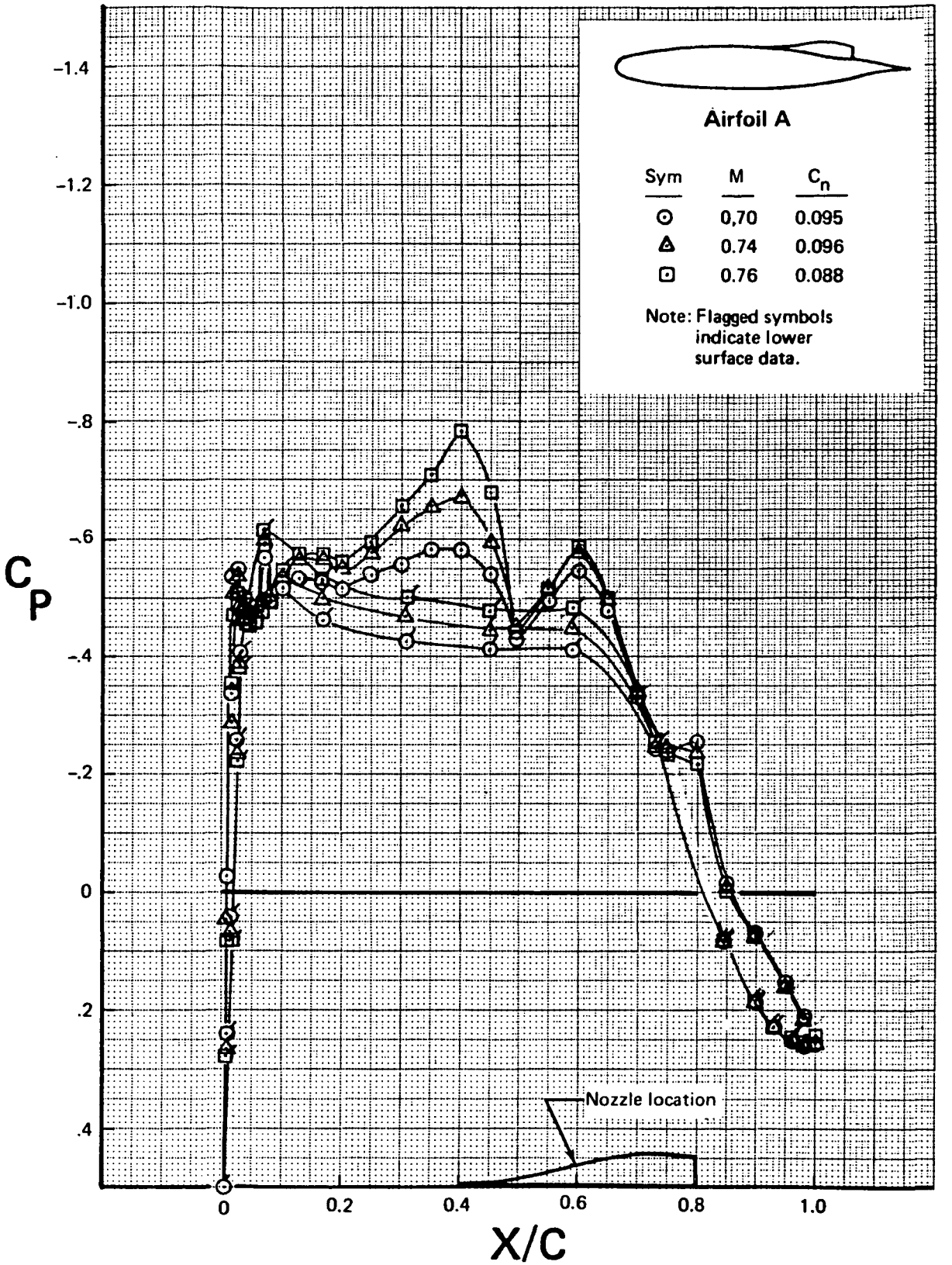

(a) $C_\mu = 0$, $\alpha_g = 1°$

Figure 10.—Effect of Change in Mach Number on Airfoil Chordwise Pressure Distribution

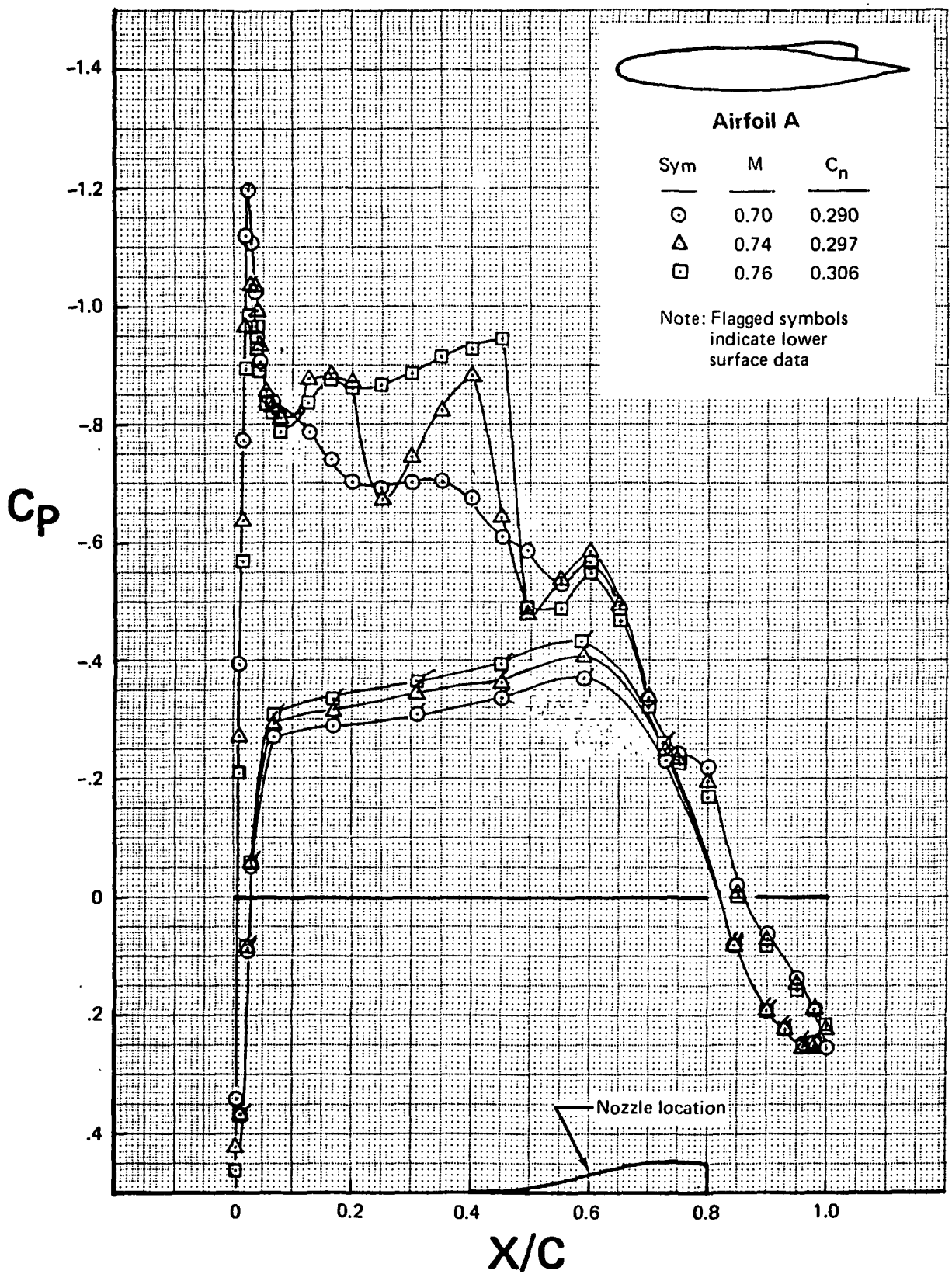

(b) $C_\mu = 0$, $\alpha_g = 3°$

Figure 10.—Continued

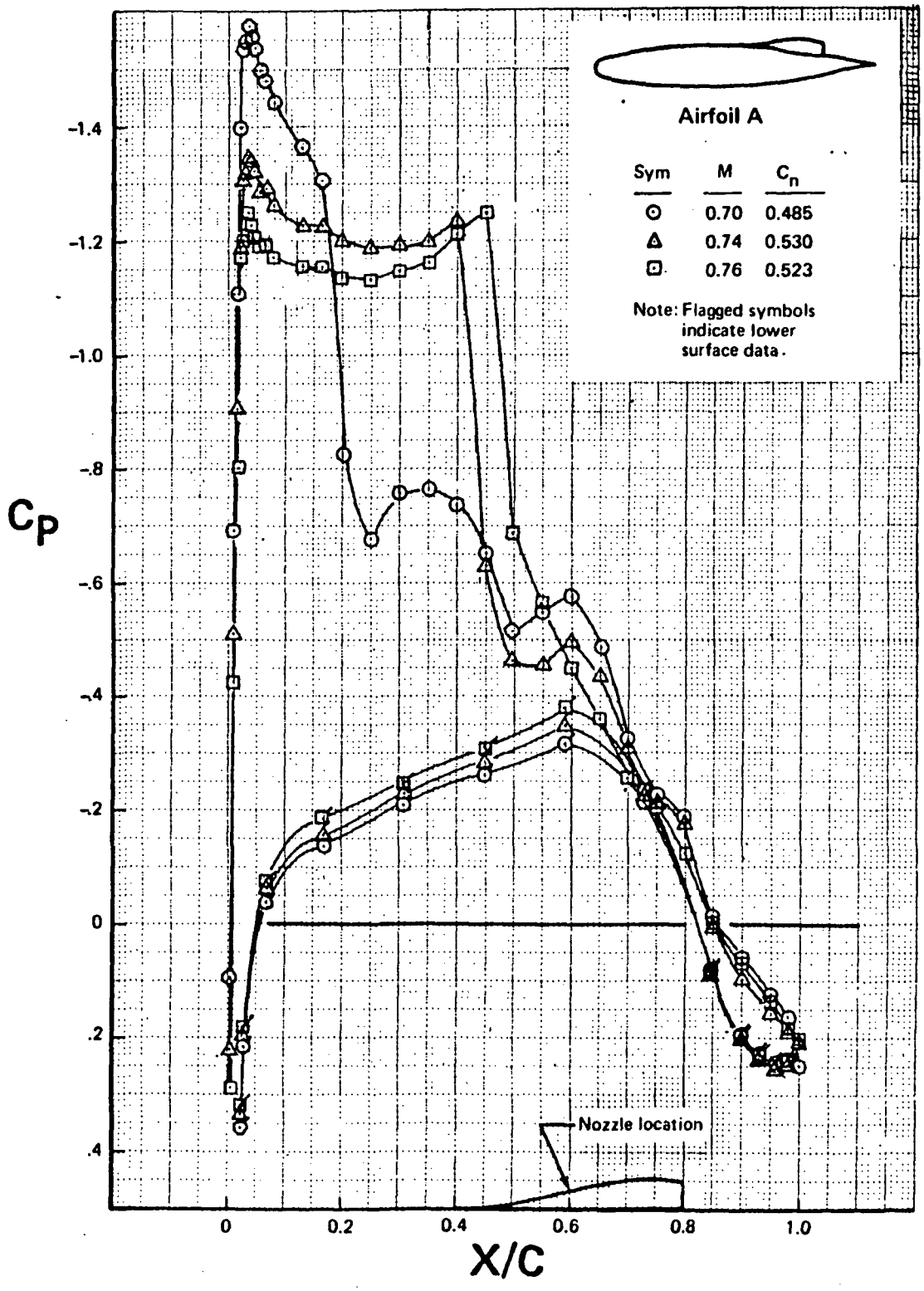

(c) $C_\mu = 0$, $\alpha_g = 5°$

Figure 10.—Continued

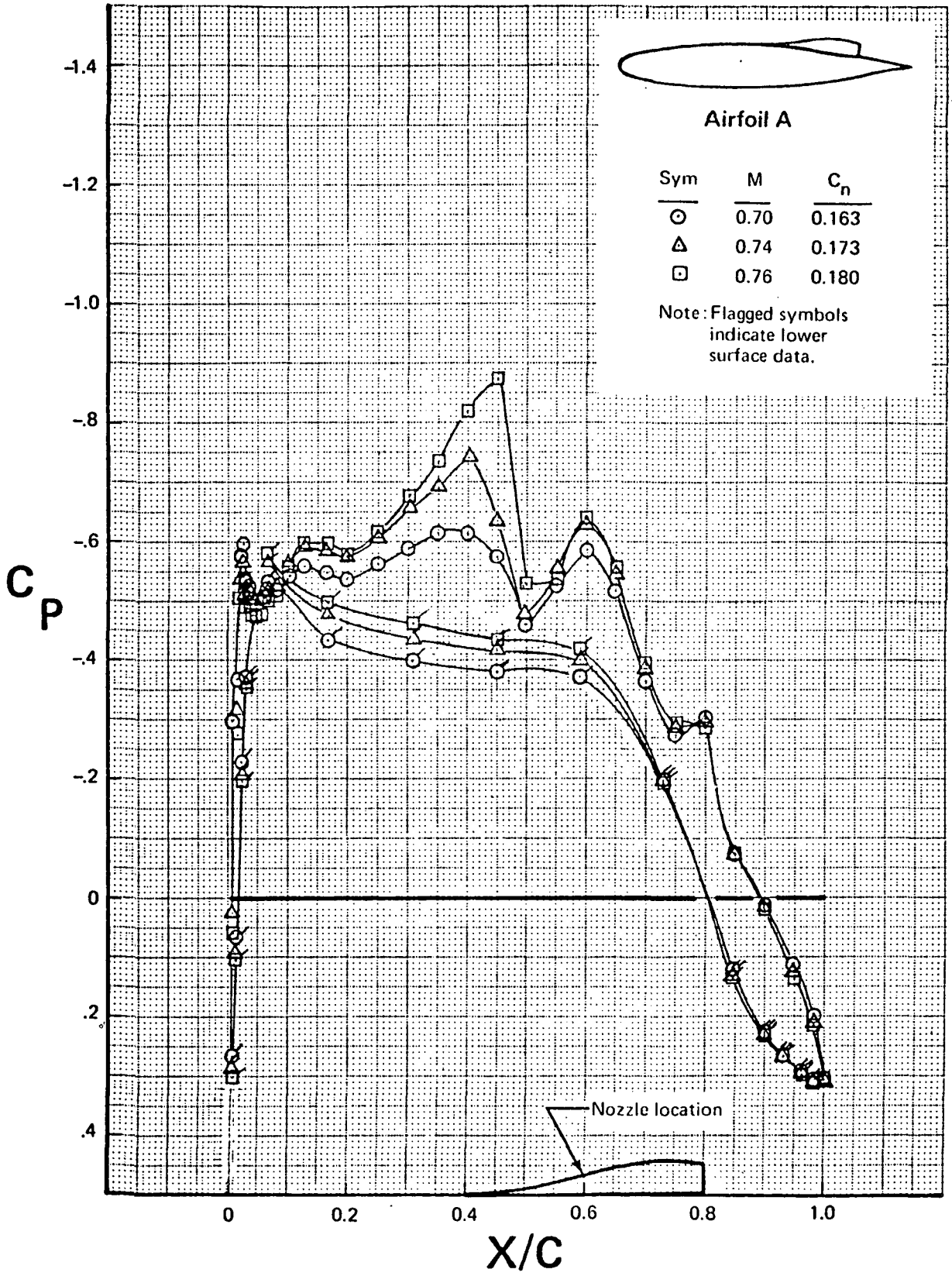

(d) $C_\mu = 0.028$, $\alpha_g = 1°$

Figure 10.—Continued

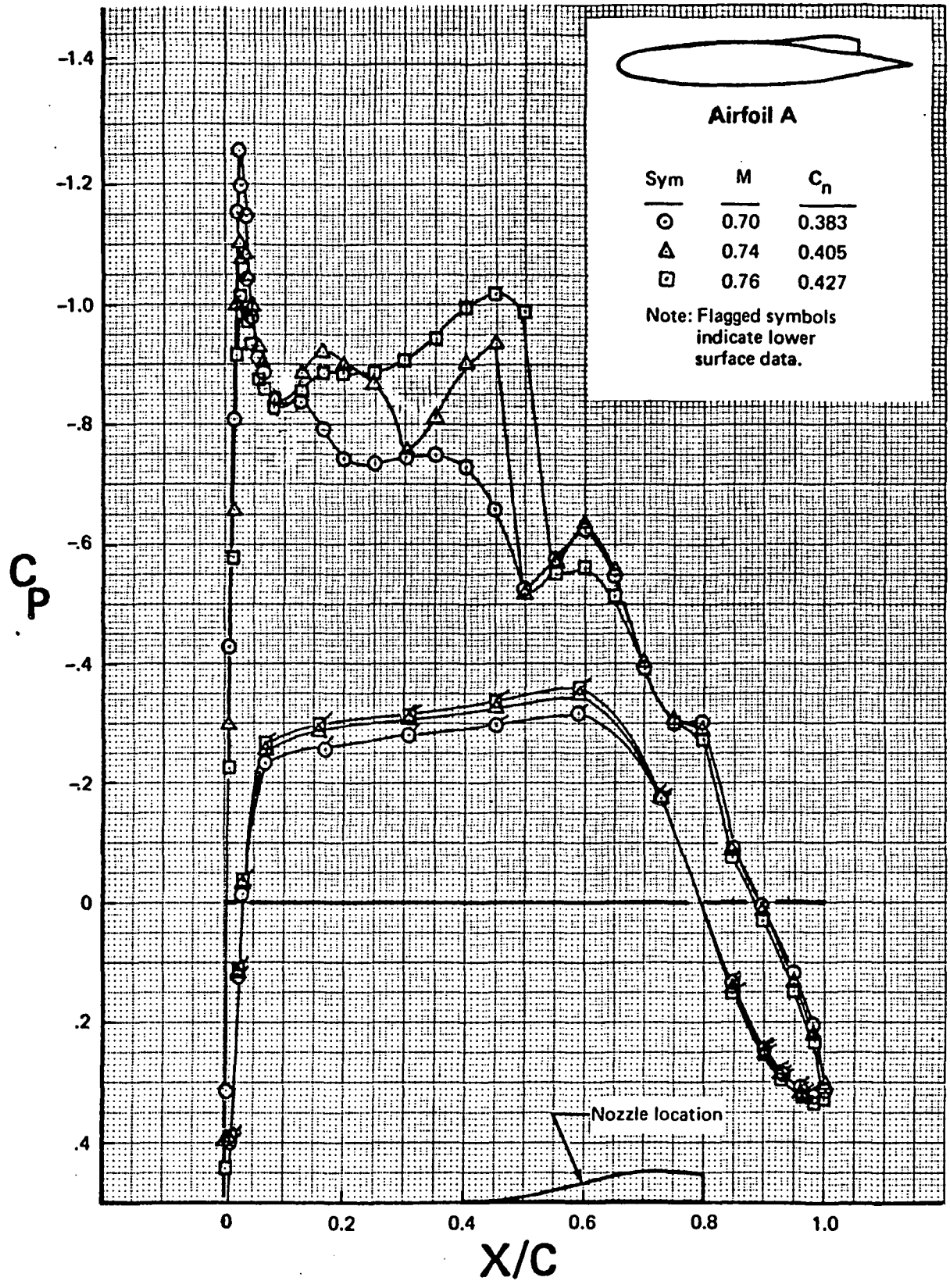

(e) $C_\mu = 0.028, \alpha_g = 3^\circ$

Figure 10.–Continued

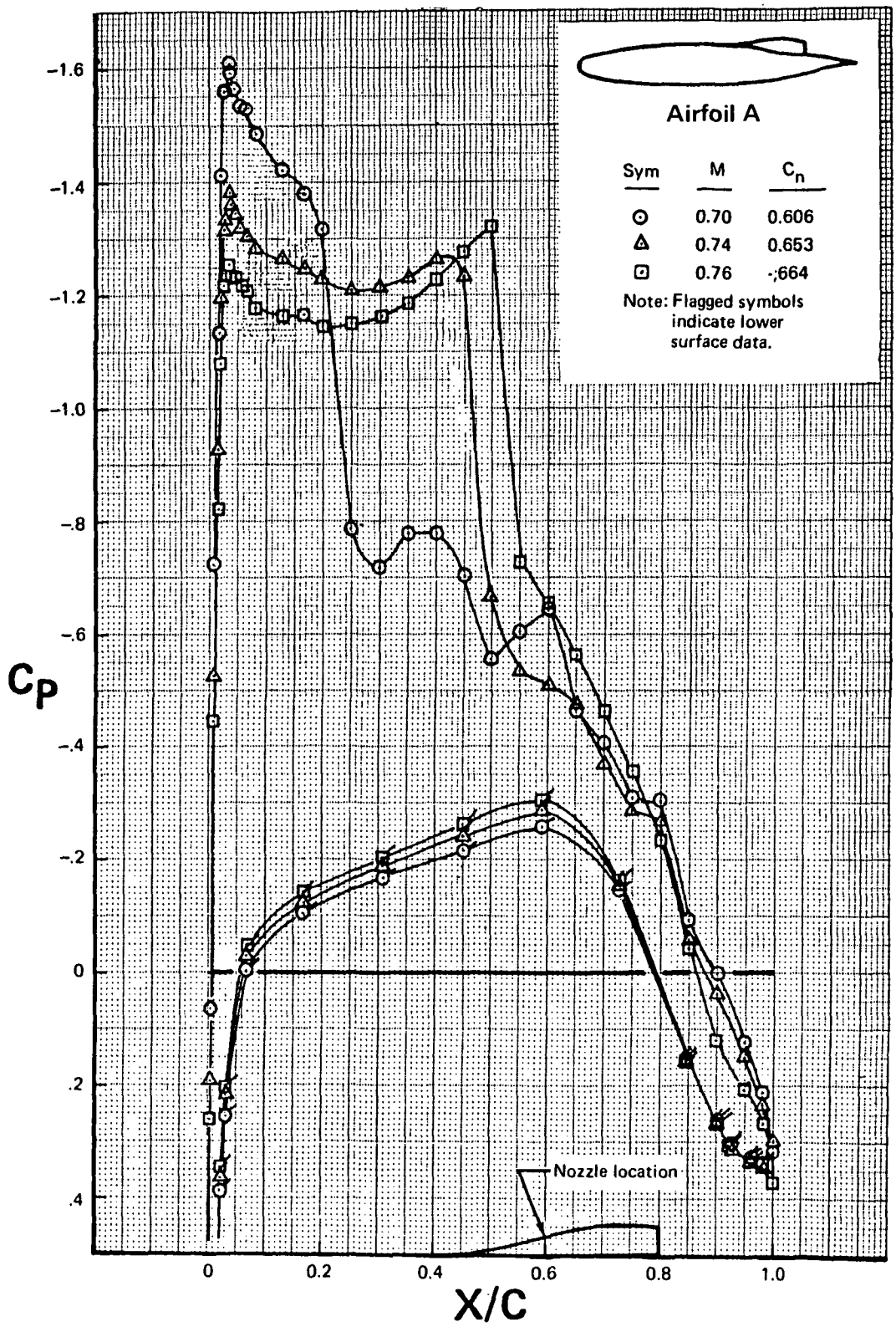

(f) $C_\mu = 0.028$, $\alpha_g = 5°$

Figure 10.—Continued

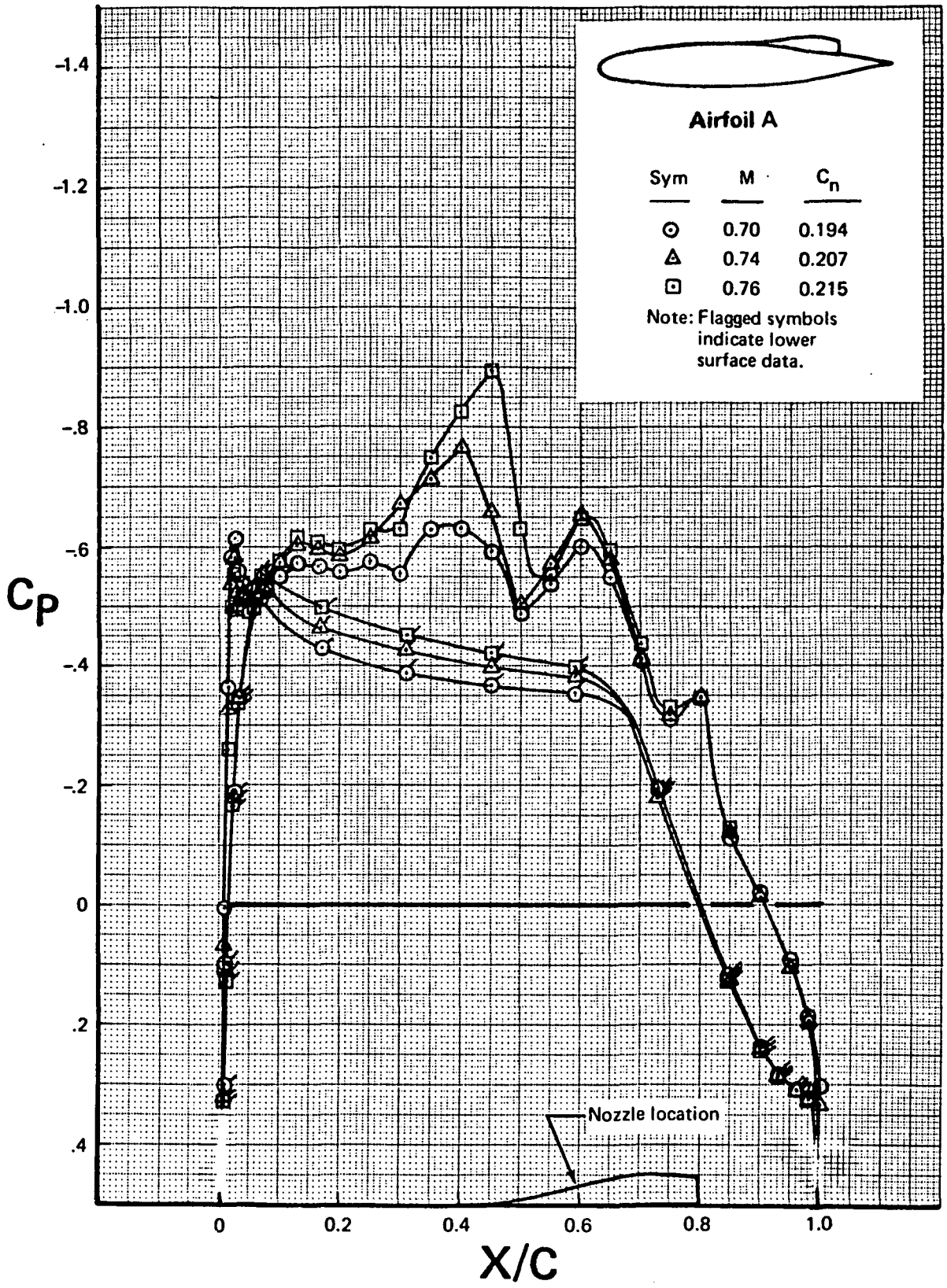

(g) $C_\mu = 0.044$, $\alpha_g = 1°$

Figure 10.—Continued

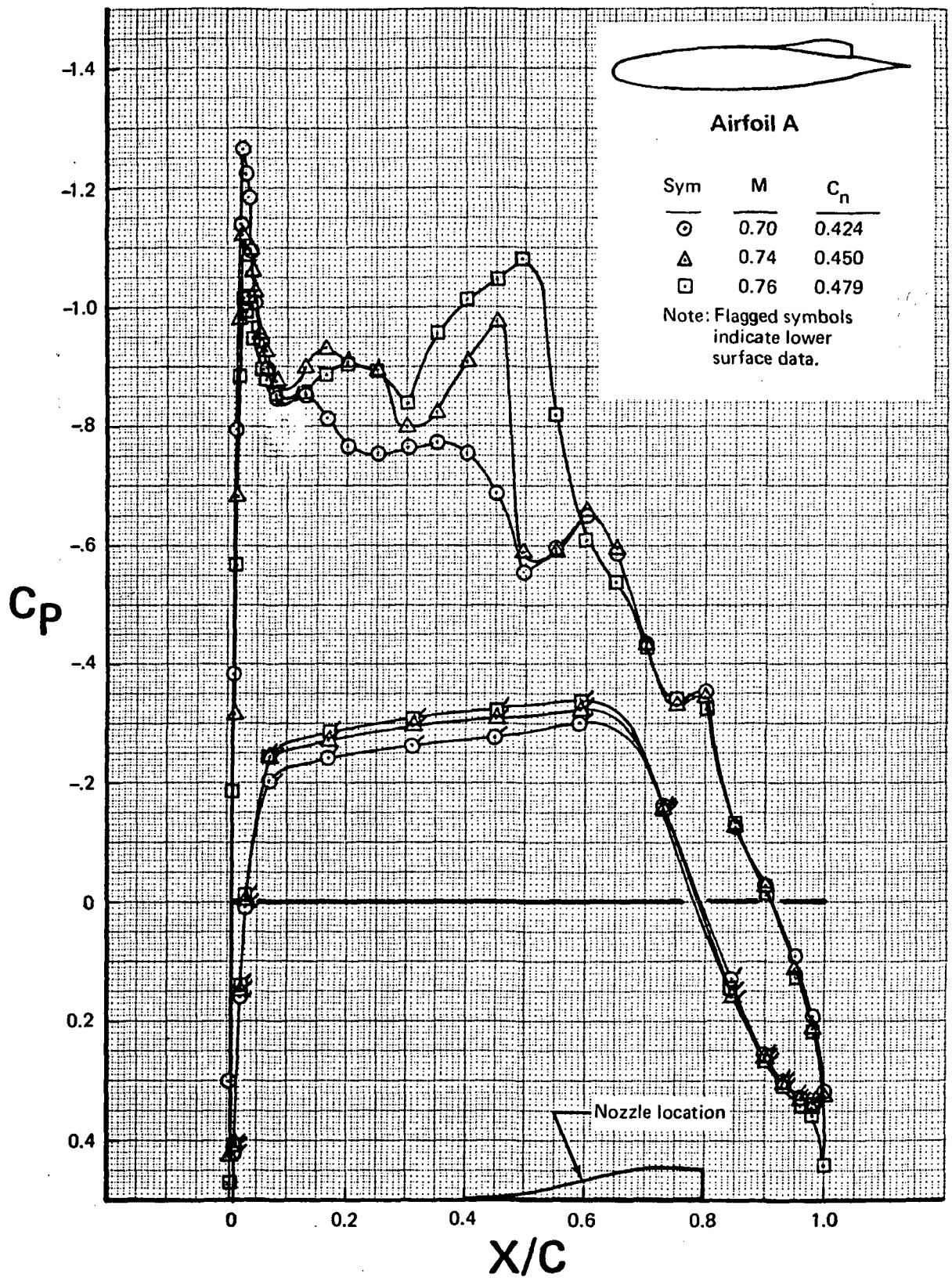

(h) $C_\mu = 0.044$, $\alpha_g = 3°$

Figure 10.—Continued

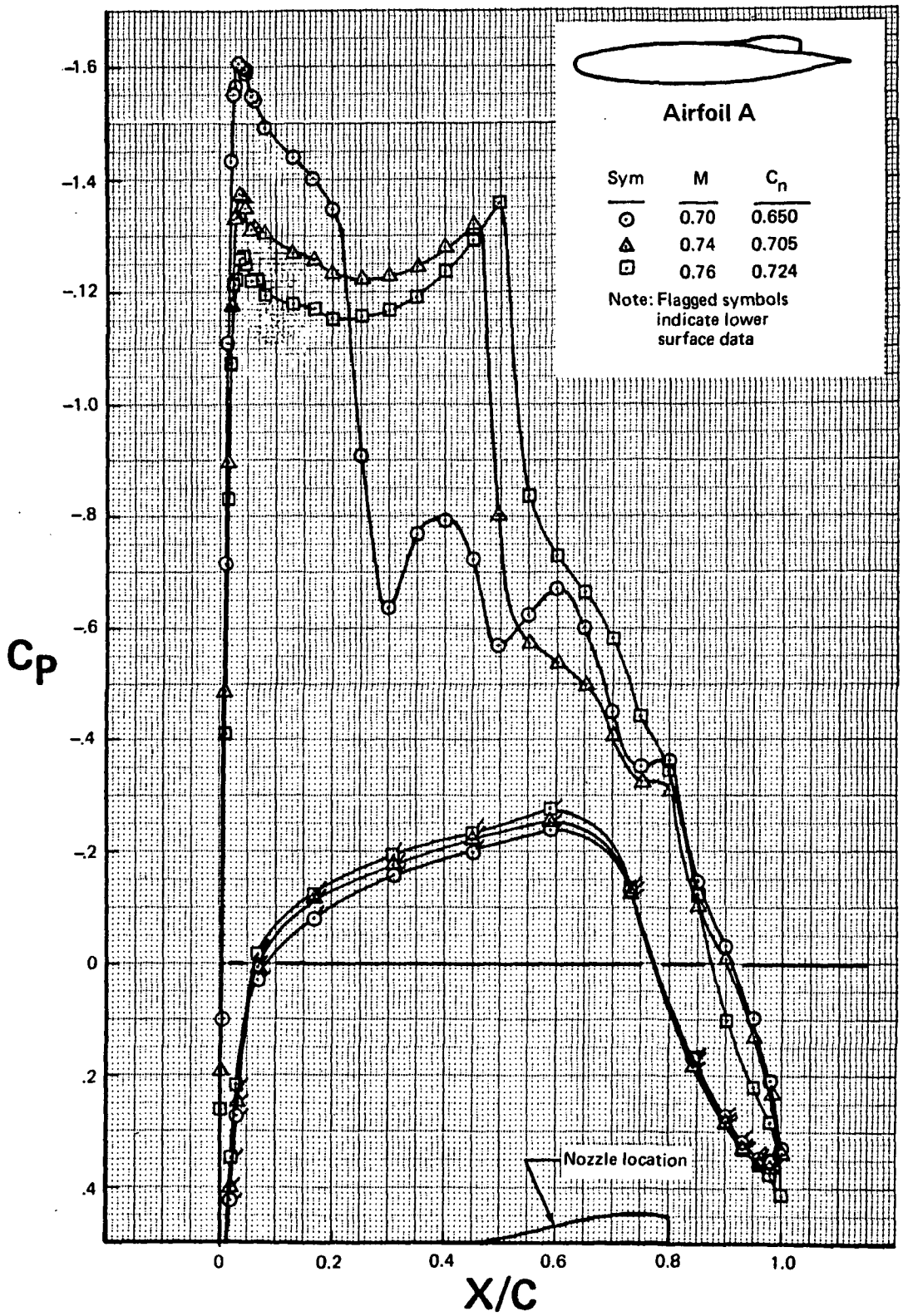

(i) $C_\mu = 0.044$, $\alpha_g = 5°$

Figure 10.—Concluded

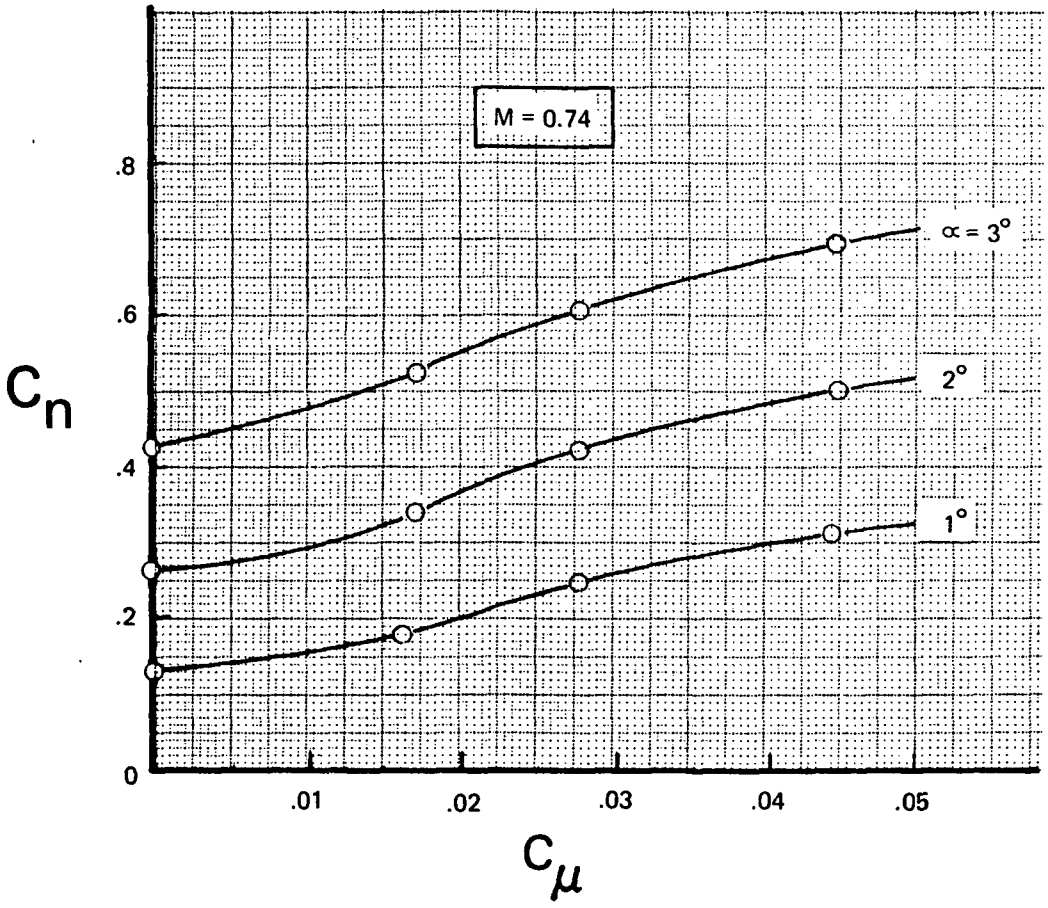

Figure 11.—Effect of Change in Blowing Momentum Coefficient on Section Normal Force Coefficient at Constant Angles of Attack

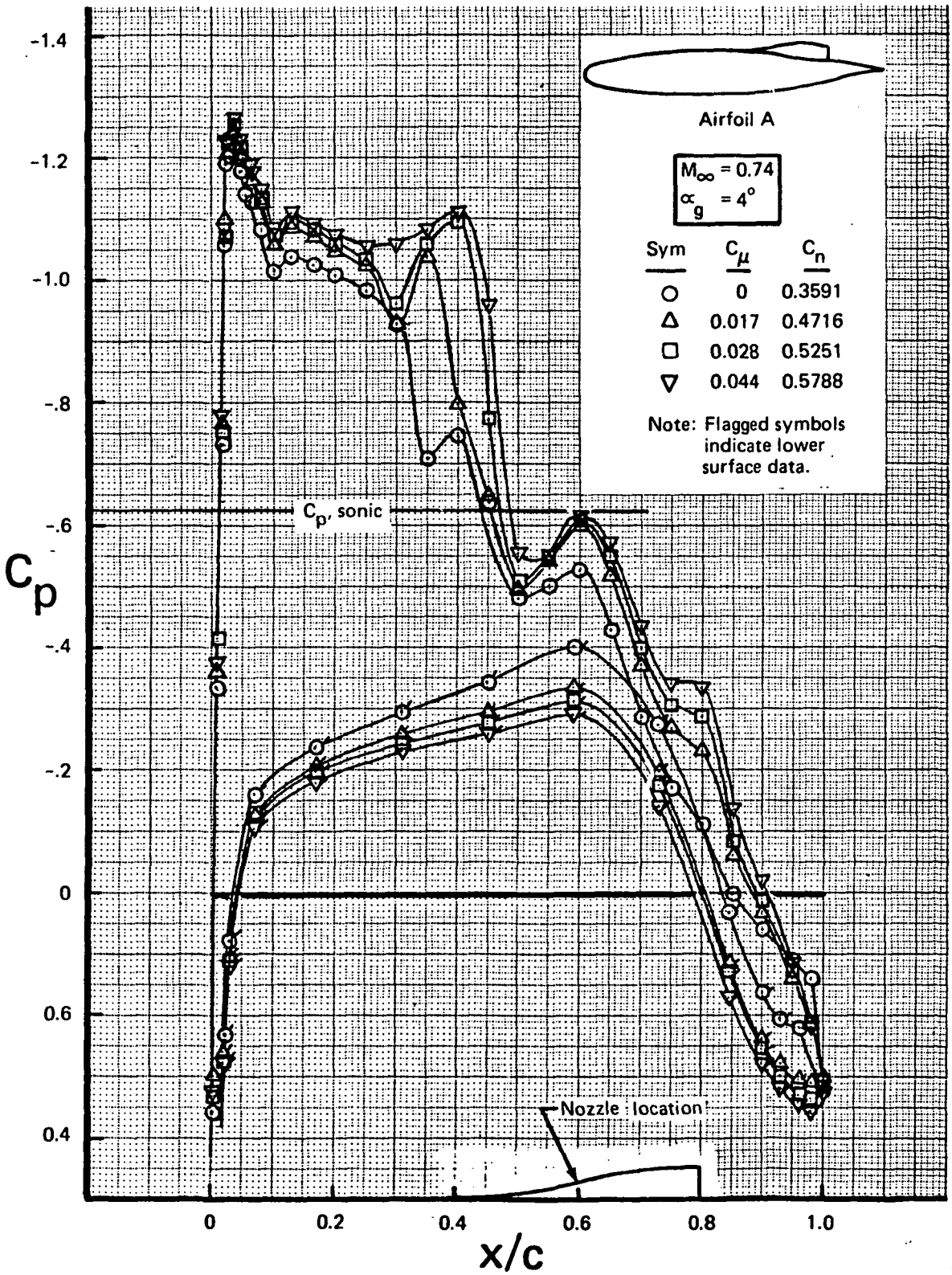

Figure 12.—Chordwise Pressure Distribution for Airfoil With Blowing Momentum Coefficient Values

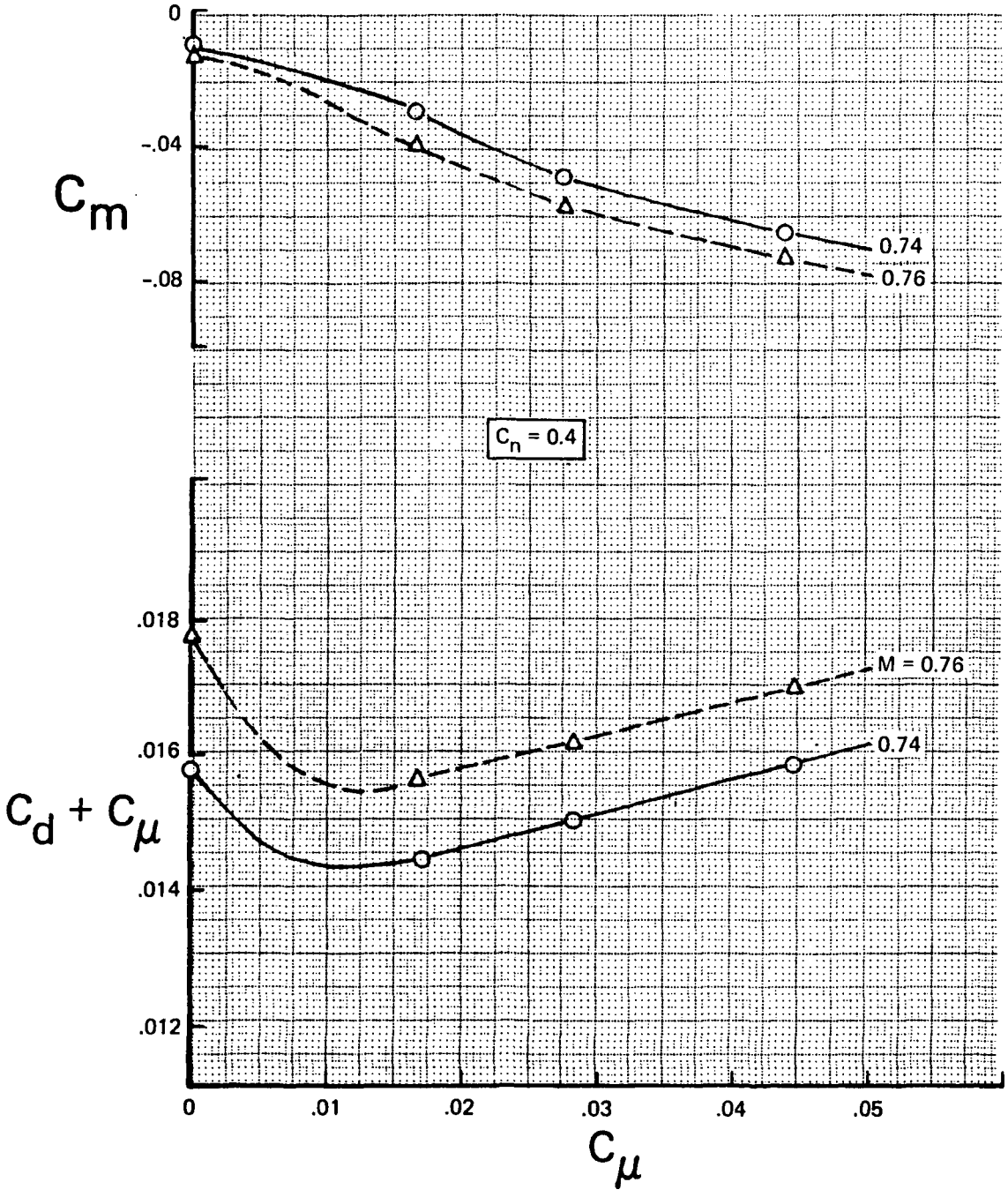

Figure 13.—Effect of Change in Blowing Momentum Coefficient on Section Effective Drag Coefficient and Pitching Moments

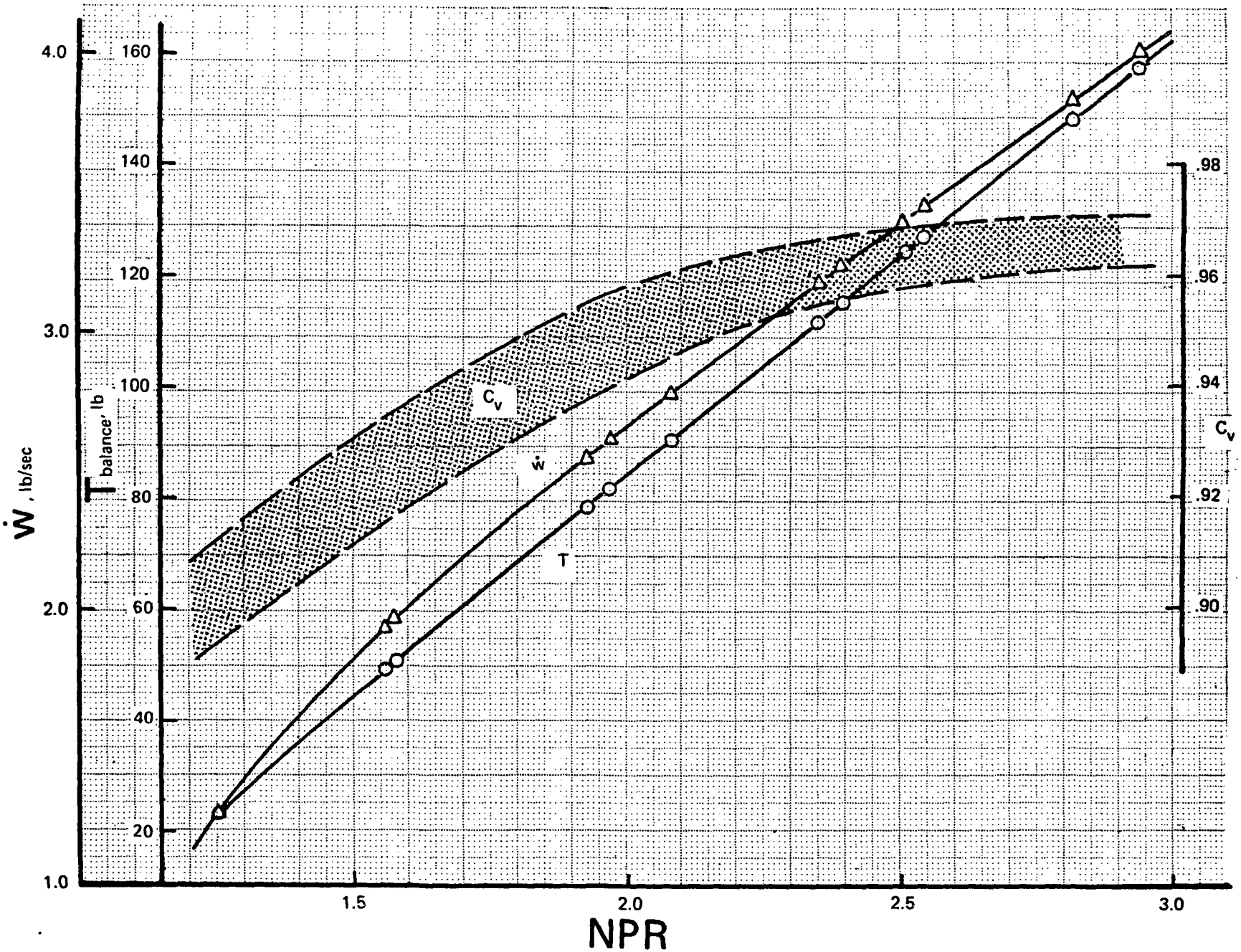

Figure 14.—Variation of Nozzle Air Weight Flow, Thrust, and Velocity Coefficient With Nozzle Exit Total Pressures at Static Conditions

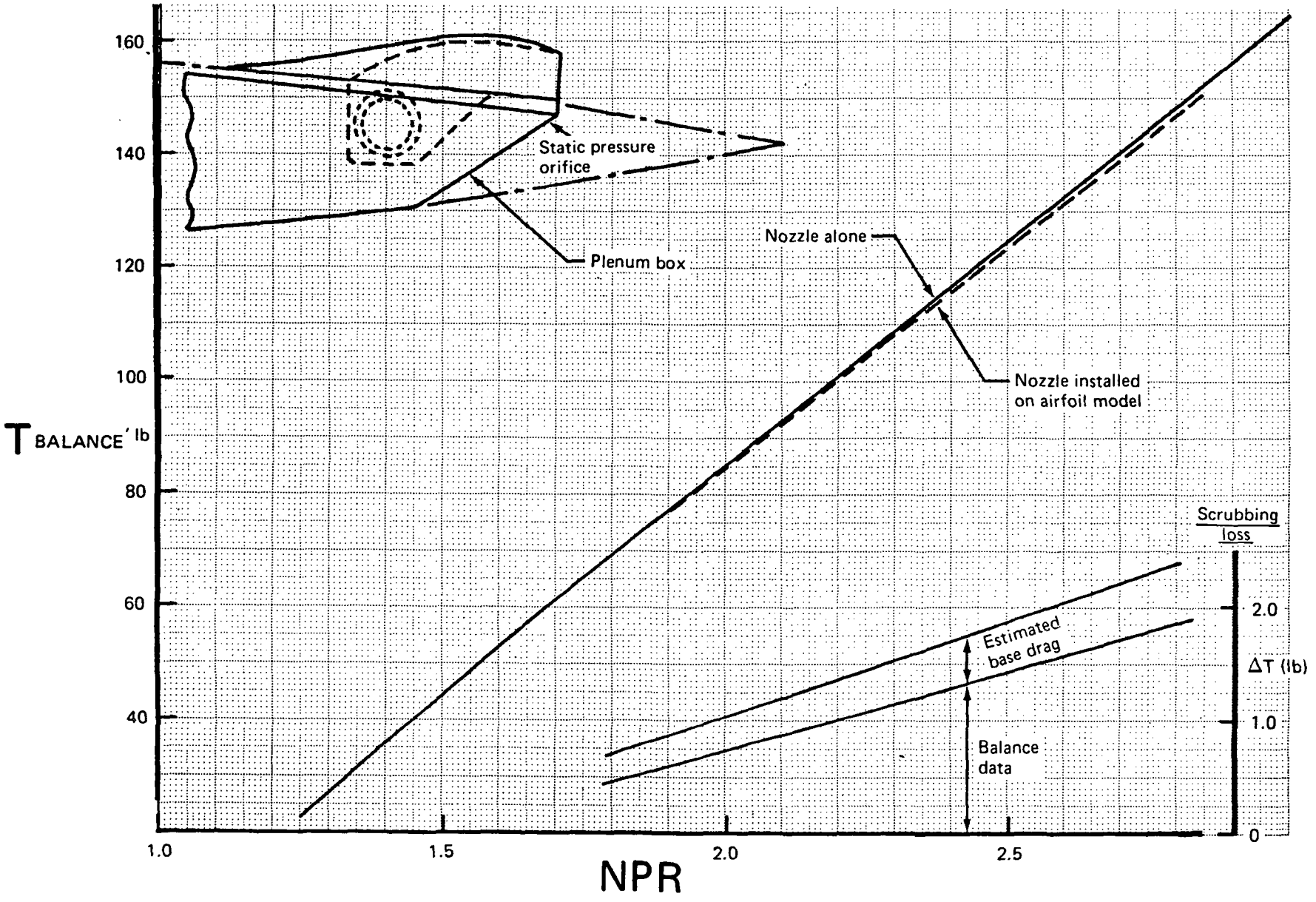

Figure 15.—Effect of Upper Surface Scrubbing of Nozzle Jet on Static Thrust

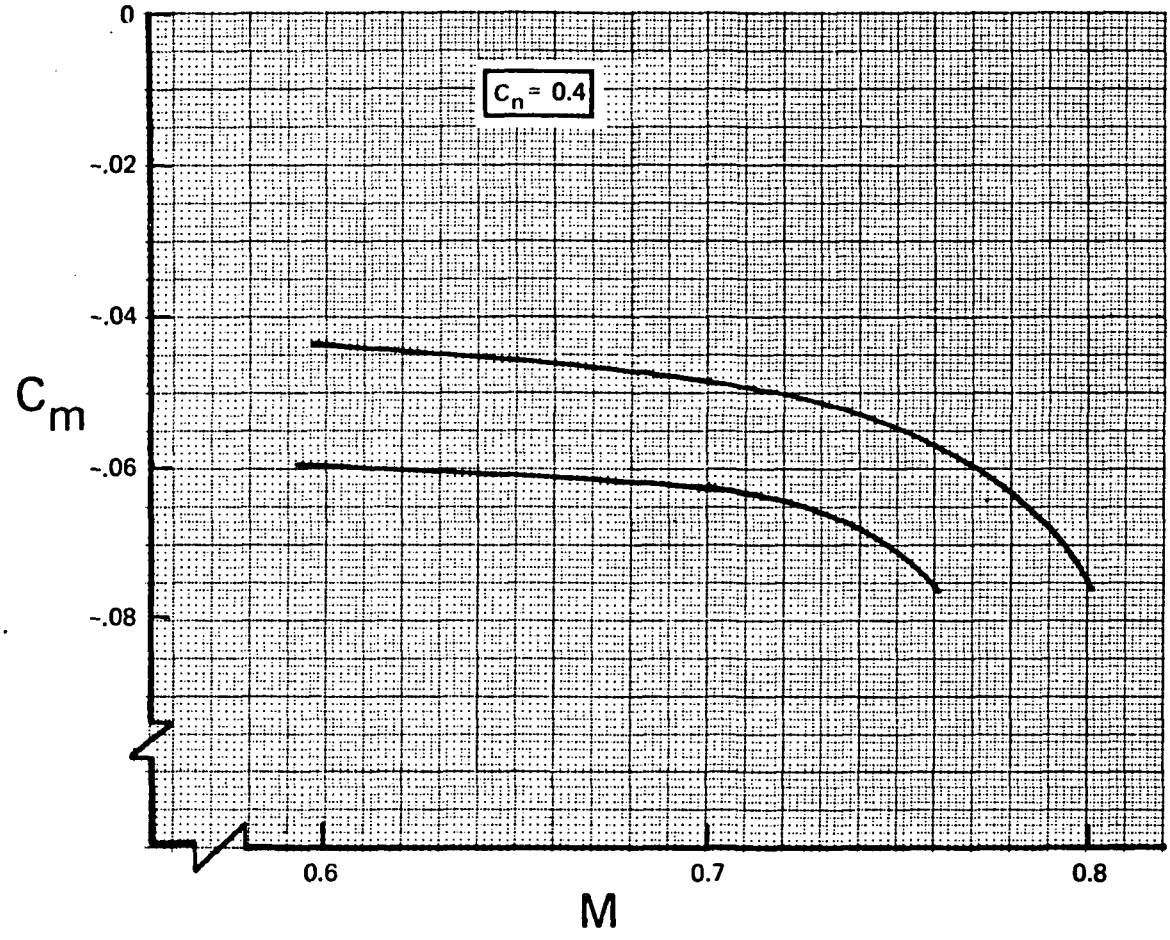

Figure 16.—Variation of Section Pitching Moment Coefficients With Mach Number

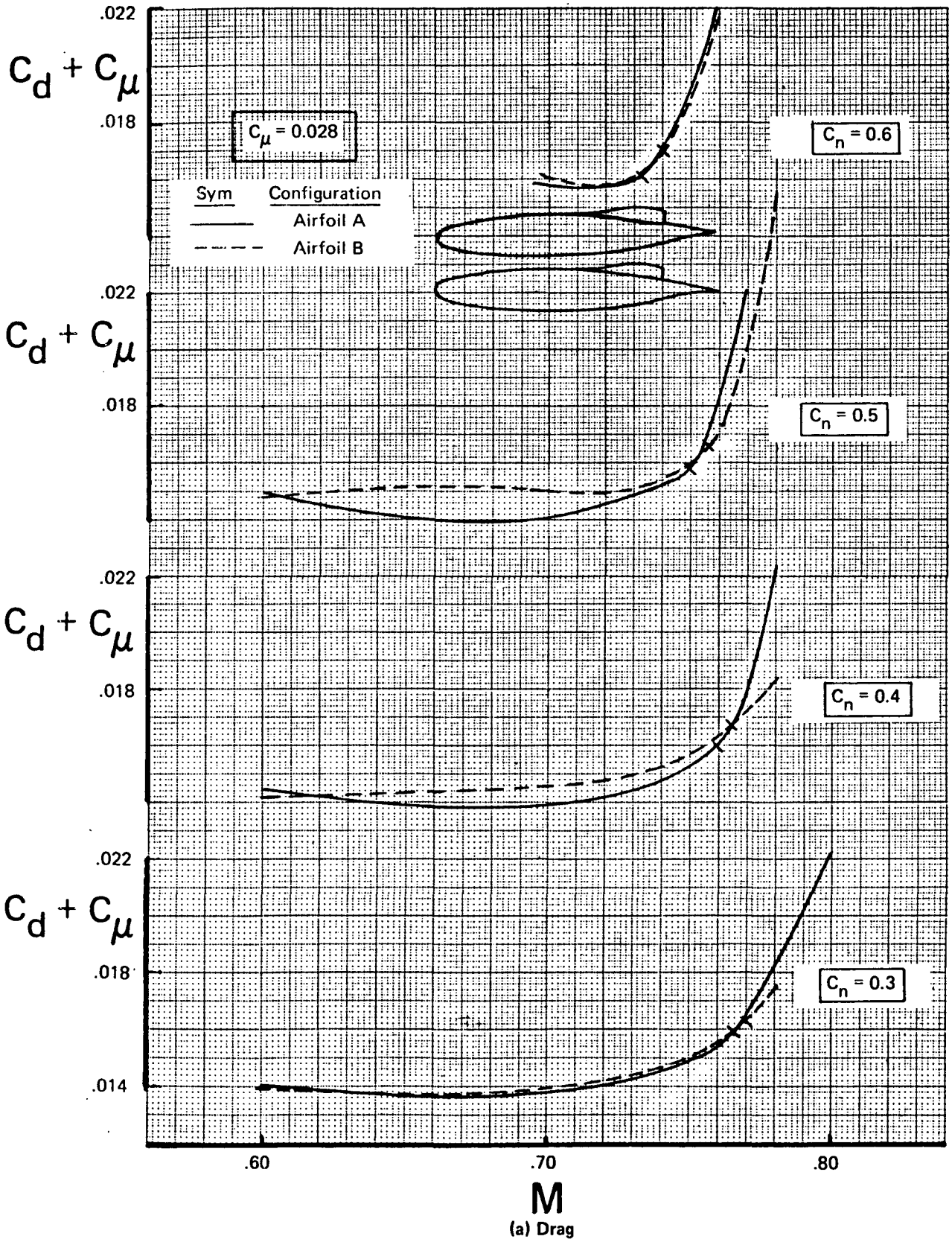

(a) Drag

Figure 17.—Effect of Area Ruling of Nozzle Channel on Drag and Surface Pressure Distribution

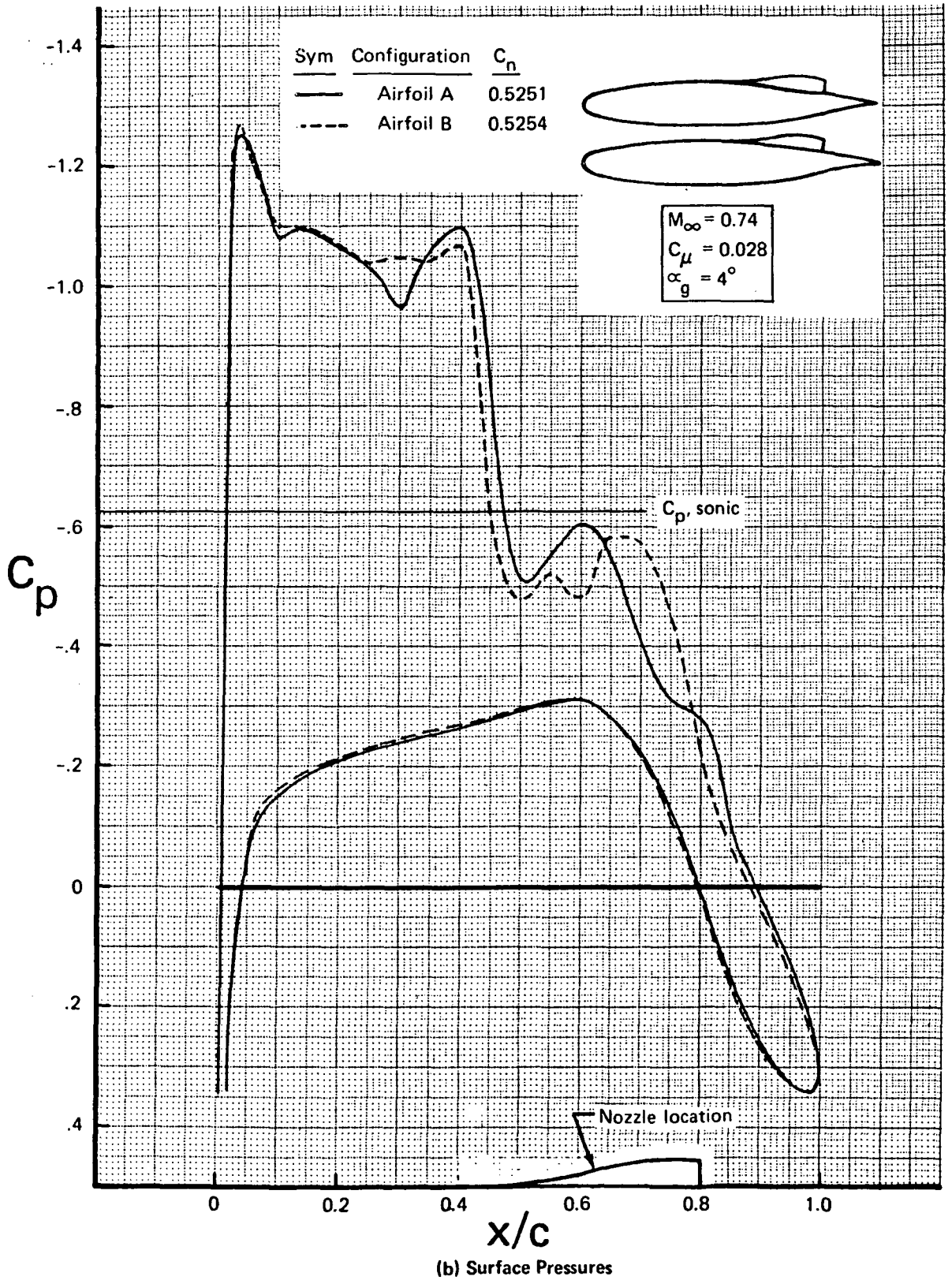

(b) Surface Pressures

Figure 17.—Concluded

1. Report No.	2. Government Accession No.	3. Recipient's Catalog No.
NASA CR-114560		

4. Title and Subtitle	5. Report Date
DESIGN INTEGRATION AND NOISE STUDIES FOR JET STOL AIRCRAFT. Task VIIB: Wind Tunnel Investigation of a 14-Percent-Thick Airfoil With Upper Surface Blowing at High Subsonic Mach Numbers	January 1973
	6. Performing Organization Code

7. Author(s)	8. Performing Organization Report No.
Avtar S. Mahal and Ian J. Gilchrist	D6-60182
	10. Work Unit No.

9. Performing Organization Name and Address	11. Contract or Grant No.
BOEING COMMERCIAL AIRPLANE COMPANY P.O. Box 3707 Seattle, Washington 98124	NAS2-6344
	13. Type of Report and Period Covered Contractor final research report June 1972–Jan 1973

12. Sponsoring Agency Name and Address	14. Sponsoring Agency Code
NATIONAL AERONAUTICS AND SPACE ADMINISTRATION Ames Research Center Moffett Field, California 94035	

15. Supplementary Notes

16. Abstract

An exploratory wind tunnel test has been conducted at Mach numbers from 0.60 to 0.80 to investigate the effects of nozzle geometry and upper surface blowing on the aerodynamic characteristics of a 14-percent-thick airfoil. Measured data included lift, drag, pitching moments, surface pressures, and nozzle thrust.

17. Key Words (Suggested by Author(s))	18. Distribution Statement
Transonic airfoil Upper surface blowing	

19. Security Classif. (of this report)	20. Security Classif. (of this page)	21. No. of Pages	22. Price*
Unclassified		43	

*For sale by the National Technical Information Service, Springfield, Virginia 22151